UNIVERSIDADE FEDERAL DE PELOTAS

Programa de Pós-Graduação em Odontologia

TESE

INFLUÊNCIA DA INCORPORAÇÃO DE NANOPARTÍCULAS E UTILIZAÇÃO DE MONÔMEROS ÁCIDOS COMO AGENTES DE UNIÃO EM CIMENTOS RESINOSOS

Luciano de Vargas Habekost

Pelotas, 2011

LUCIANO DE VARGAS HABEKOST

INFLUÊNCIA DA INCORPORAÇÃO DE NANOPARTÍCULAS E UTILIZAÇÃO DE MONÔMEROS ÁCIDOS COMO AGENTES DE UNIÃO EM CIMENTOS RESINOSOS

Tese apresentada ao Programa de Pós-Graduação em Odontologia, Área de concentração em Dentística, da Faculdade de Odontologia da UNIVERSIDADE FEDERAL DE PELOTAS, como requisito parcial à obtenção do título de Doutor em Odontologia.

Orientador: Prof. Dr. Guilherme Brião Camacho
Co-orientadores: Profª. Drª. Giana da Silveira Lima
Prof. Dr. Rafael Ratto de Moraes

Pelotas, 2011

Banca examinadora:

Prof. Dr. Guilherme Brião Camacho (Orientador)

Prof. Dr. Bruno Lopes da Silveira

Profª. Drª. Márcia Bueno Pinto

Prof. Dr. Renato Fabrício de Andrade Waldemarin

Profª. Drª. Tatiana Pereira Cenci

Profª. Drª. Adriana Fernandes da Silva (Suplente)

Prof. Dr. Fábio Garcia Lima (Suplente)

DEDICATÓRIA

Dedico este trabalho:

A **Deus**,
Que em momentos difíceis segurou minha mão e mostrou o caminho!

Aos meus pais **Zemir** e **Maria Lúcia**,
Que, com todo o amor, dedicam suas vidas aos seus filhos!
Obrigado por estar aqui e participar de suas vidas!
Amo vocês!

A minha linda e amada esposa **Ana Cláudia**,
Que me mostrou um novo e maravilhoso mundo!
Obrigado pelos sorrisos, pelo carinho e pela atenção!

A minha irmã **Simone** e ao meu cunhado **Cleiton**,
Que, além de serem companheiros em todas as horas,
colocaram a **Sofia** em nossas vidas!

A minha dinda **Círis** e a minha vovó **Noeli**,
Que sempre estão torcendo por mim!

AGRADECIMENTOS

As famílias **Vargas** e **Habekost,** que são a base do que sou hoje!

Aos meus sogros **Cláudio** e **Vera**, pela ajuda em todos os momentos! Missão dada é missão cumprida!

Ao meu orientador **Professor Doutor Guilherme Camacho,** minha gratidão pela amizade, confiança depositada e conhecimentos transmitidos! Que sempre possamos continuar compartilhando conhecimentos dentro e fora do maravilhoso mundo da prótese!

A minha co-orientadora **Professora Doutora Giana da Silveira Lima,** pela dedicação de forma integral à realização deste trabalho! Tua dedicação e amizade aos alunos é exemplo para quem deseja seguir a docência!

Ao meu co-orientador **Professor Doutor Rafael Ratto de Moraes** que, com sua incrível capacidade de organizar idéias, aperfeiçoou este trabalho de forma admirável! Serei sempre grato à tua dedicação!

Ao **Professor Doutor Flávio Fernando Demarco**, por abrir meus horizontes demonstrando que a odontologia é bem mais que um consultório! Obrigado por repartir conosco a sua genialidade!

Aos **Professores Doutores Fabrício Aulo Ogliari** e **Evandro Piva,** que ajudaram um protesista a entrar no mundo dos materiais dentários! Admiro vocês pela capacidade e entusiasmo com que produzem ciência!

A minha colega **Glória,** obrigado pela colaboração na execução dos trabalhos!

Ao **Programa de Pós-Graduação em Odontologia / UFPel,** que amplia de forma singular o nosso modo de analisar, não somente a odontologia, mas nossas vidas!

“O futuro pertence àqueles que acreditam na beleza de seus sonhos.”

Elleanor Roosevest

NOTAS PRELIMINARES

A presente tese foi redigida segundo o Manual de Normas para Dissertações, Teses e Trabalhos Científicos da Universidade Federal de Pelotas de 2006, adotando o Nível de Descrição 4 – estruturas em Artigos, que consta no Apêndice D do referido manual. Disponível no endereço eletrônico:
http://www.ufpel.tche.br/prg/sisbi/documentos/Manual_normas_UFPel_2006.pdf

RESUMO

HABEKOST, Luciano de Vargas. **Influência da incorporação de nanopartículas e da utilização de monômeros ácidos como agentes de união em cimentos resinosos odontológicos.** 2011. 94f. Tese (Doutorado). Programa de Pós-graduação em Odontologia, Universidade Federal de Pelotas, Pelotas - RS, Brasil.

O objetivo deste estudo foi investigar a influência da incorporação de nanopartículas e o uso de silano (TSPM), monômero ácido fosfatado (PAM) ou monômero ácido carboxilado (CAM) como agentes de união nas propriedades de cimentos resinosos experimentais. Uma matriz resinosa fotopolimerizável modelo foi desenvolvida com 50% de Bis-GMA e 50% de TEGDMA. Para observar o comportamento da incorporação de nanopartículas, cinco cimentos resinosos experimentais foram preparados pela adição de 60% (em massa) de micropartículas de bário borosilicato de vidro (2µm) e nanopartículas de sílica coloidal (7nm). As nanopartículas foram utilizadas nas seguintes proporções (em massa): 0 (controle), 1 (G1), 2.5 (G2.5), 5 (G5) e 10% (G10). Para estudar a influência dos agentes de união, 60% (em massa) de partículas inorgânicas (59/1 de micro/nanopartículas) de vidro de Ba-B-Al-Si e sílica coloidal, cobertas com 5% de TSPM, PAM ou CAM, foram acrescidas à matriz resinosa; o grupo controle foi composto por partículas não tratadas. As propriedades avaliadas foram resistência flexural (σ), módulo de elasticidade (E_f), número de dureza Knoop (KHN) e espessura de película (FT). A dispersão/interação das partículas com a fase resinosa foi avaliada com microscópio eletrônico de varredura (MEV). O grau de conversão (DC) foi avaliado somente para estudar a influência dos diferentes agentes de união. Os dados foram submetidos à análise estatística (5%). Resultados para incorporação de nanopartículas: para σ, G1 > G2.5 = G5 = G10 e controle > G10. Para E_f, G2.5 > controle = G1 > G5 > G10. Para KHN, G5 = G10 > controle = G1 = G2.5. Para FT, controle = G1 < G5 = G10 e G2.5 < G10. Nas análises em MEV, a presença de aglomerados foi associada à incorporação de nanopartículas. Resultados para a utilização de diferentes agentes de união: para σ

e E_f, TSPM > CAM > controle > PAM. Para KHN, TSPM > CAM > PAM = controle. Para FT, TSPM < controle < CAM < PAM. As análises em MEV revelaram aglomerados de nanopartículas em todos os grupos e melhor interação entre as fases orgânica/inorgânica para TSPM e CAM. Não foram observadas diferenças para o DC. Os resultados demonstraram que a incorporação moderada de nanopartículas de sílica silanizada pode beneficiar as propriedades dos cimentos resinosos híbridos. Entretanto, proporções de nanopartículas acima de 2,5% possuem um efeito prejudicial nas propriedades destes cimentos, e seu aumento está associado com o aumento da presença de aglomerados. O uso de TSPM gerou cimentos com melhores propriedades quando comparado ao uso de monômeros ácidos, o CAM demonstrou melhor desempenho que o PAM. O uso do PAM gerou cimentos com propriedades inferiores a cimentos sem a utilização de agentes de união.

Palavras-chave: Agente de união. Cimento resinoso. Monômero ácido. Nanopartículas. Silano.

ABSTRACT

HABEKOST, Luciano de Vargas. **Influence of nanoparticle incorporation and use of acidic monomers as coupling agents in dental resin luting agents**. 2011. 94p. Thesis (Doctorate) – Post Graduate Program, School of Dentistry, Federal University of Pelotas, Pelotas - RS, Brazil.

The objective of this study was to investigate the influence of nanoparticle loading and the use of silane (TSPM), phosphate (PAM) or carboxylic (CAM) methacrylates as coupling agents on key properties of experimental resin luting agents. An experimental photocurable resin blend composed with 50 wt% of Bis-GMA and 50 wt% of TEGDMA was obtained. To study the influence nanoparticle loading, five different experimental resin luting agents were prepared with a total mass fraction of 60% of inorganic fillers. Silanated 2-µm barium borosilicate glass microparticles and 7-nm silica nanoparticles were used; the mass fraction of nanoparticles was set at 0 (control), 1 (G1), 2.5 (G2.5), 5 (G5) and 10% (G10). To study the influence of coupling agents, the resin blend was loaded with a 60% mass fraction of inorganic fillers (59/1 mass ratio of micro/nanoparticles) of Ba-B-Al-Si glass and colloidal silica coated with 5 wt% of TSPM, PAM or CAM; no filler treatment was performed in the control group. The properties evaluated were flexural strength (σ) and modulus (E_f), Knoop hardness number (KHN), and film thickness (FT). Dispersion/interaction of particles with the resin phase was assessed by scanning electron microscopy (SEM). The degree of conversion (DC) was evaluated only to study the influence of coupling agents. Data were submitted to statistical analysis (5%). Results for nanoparticle loading: for σ, G1 > G2.5 = G5 = G10, and control > G10. For E_f, G2.5 > control = G1 > G5 > G10. For KHN, G5 = G10 > control = G1 = G2.5. For FT, control = G1 < G5 = G10, and G2.5 < G10. Incorporation of nanoparticles was associated with observation of clusters in the SEM analysis. Results for different coupling agents: for σ and E_f, TSPM > CAM > control > PAM. For KHN, TSPM > CAM > PAM = control. For FT, TSPM < control < CAM < PAM. The SEM analysis revealed clustering of nanoparticles for all groups and better interaction between the organic-inorganic

phases for TSPM and CAM. No significant differences in DC were observed. The results demonstrated that moderate incorporation of silanated silica nanoparticles may improve the properties of hybrid resin cements. However, mass fraction above 2.5% had a detrimental effect on the luting agent properties and the increase of clusters is associated with the increase of nanoparticles. The use of TSPM generated agents with improved properties as compared with the acidic methacrylates, with CAM showing better performance than PAM. The use of PAM generated agents with properties usually poorer compared with the material with no coupling agent.

Keywords: Acid monomer. Coupling agent. Nanoparticles. Resin luting agent. Silane.

LISTA DE ABREVIATURAS

%	Por cento
Al	Alumínio
ANOVA	Análise de variância
ATR	Refletância total atenuada
B	Boro
Ba	Bário
Bis-GMA	Éster do bisfenol-A com dimetacrilato de glicidila
CAM	Monômero ácido carboxilado
CDC-Bio	Centro de Desenvolvimento e Controle de Biomateriais
cm	Centímetro
cm^2	Centímetro quadrado
CT	Connecticut
DC	Grau de conversão
E	Módulo de elasticidade
EUA	Estados Unidos da América
FT	Espessura de película
FTIR	Infravermelho por Transformada de Fourier
g	Grama
GPa	Gigapascal
h	Hora
IL	Ilinóis
ISO	Organização Internacional de Padronização
kgf	Quilograma-força
KHN	Número de dureza Knoop
kV	Quilovolt
LED	Diodo emissor de luz
MEV	Microscópio eletrônico de varredura
min	Minuto
mL	Mililitro
mm	Milímetro
mm^2	Milímetro quadrado

MO	Missouri
MPa	Megapascal
mW	Miliwatt
N	Newton
nm	Nanometro
ºC	Graus Celsius
PA	Pensilvânia
PAM	Monômero ácido fosforado
pH	Potencial hidrogeniônico
pKa	Constante de ionização
PR	Paraná
s	Segundo
SD	Desvio padrão
SEM	Microscópio eletrônico de varredura
Si	Silício
SP	São Paulo
T	Tensão
TEGDMA	Dimetacrilato de trietilenoglicol
TSPM	Silano
UFPel	Universidade Federal de Pelotas
wt%	Percentual em massa
ε	Deformação linear
µm	Micrometro
σ	Resistência à flexão

SUMÁRIO

1 PROJETO DE TESE

1.1 INTRODUÇÃO

Os cimentos resinosos são constituídos de uma matriz resinosa carregada com partículas de reforço, com um agente de união entre ambos. O desempenho destes cimentos é dependente da soma das propriedades da matriz resinosa com as propriedades das partículas de carga, bem como da adesão entre elas promovida pelo agente de união. O cimento deve se comportar como um corpo único e, quando submetido a tensões, estas devem ser distribuídas da matriz, através da interface matriz/partícula, até a partícula de carga (Mohsen e Craig, 1995; Lin, Lee *et al.*, 2000).

Nanopartículas são caracterizadas por apresentar tamanhos entre 0,1 e 100 nanômetros e têm sido incorporadas aos cimentos resinosos, em pequenas quantidades, objetivando melhorar suas propriedades mecânicas (Mitra, Wu *et al.*, 2003). Estas partículas teriam a capacidade de preencher espaços entre as partículas maiores, permitindo a incorporação de maior volume de partículas e contribuindo para a redução da contração de polimerização (Wilson, Zhang *et al.*, 2005). O preenchimento dos espaços entre as partículas maiores resultaria no aumento dos obstáculos para propagação de trincas e na diminuição de pontos de concentração de tensão (Kim, Kim *et al.*, 2007).

Entretanto, o aumento do volume de partículas acima de certo limite tem sido relacionado à diminuição das propriedades mecânicas dos compósitos. Isto ocorreria devido ao maior número de defeitos incorporados ao material durante a mistura, aumentando a porosidade (Ikejima, Nomoto *et al.*, 2003; Tian, Gao *et al.*, 2008). Além disso, as nanopartículas, devido ao seu pequeno tamanho, proporcionariam formação de agregados de aproximadamente 5μm, onde a matriz resinosa não consegue penetrar, agindo como bolhas no interior do cimento (Lim, Ferracane *et al.*, 2002; Drummond, 2008). Outro fator a ser considerado é o aumento da viscosidade

do cimento resinoso com o aumento do volume de partículas (Drummond, 2008). Desta forma, embora o emprego de nanopartículas na formulação de cimentos resinosos seja difundido, não estão definidas em que proporções sua incorporação trará benefícios ou prejuízos às propriedades dos cimentos.

Em muitos compósitos dentais a principal causa de falha esta localizada na interface entre a partícula de carga e a matriz resinosa (Drummond, 2008). A interação partícula/matriz altera a dispersão das partículas na matriz e a união entre ambas, acarretando possível alteração em propriedades como conversão, viscosidade, espessura de película, resistência mecânica, módulo de elasticidade e dureza. Com o aumento da interação entre partículas e matriz é esperado o aumento das propriedades mecânicas do cimento quando submetido a tensões, levando a melhor transferência de carga, maior rigidez e resistência ao desgaste (Mohsen e Craig, 1995; Lim, Ferracane *et al.*, 2002). Restaurações cerâmicas apresentaram melhores resultados de resistência à fratura quando cimentadas com cimentos resinosos com maior módulo de elasticidade, devido à maior capacidade destes de transferir tensões das restaurações para a estrutura dentária (Habekost, Camacho *et al.*, 2007).

Enquanto as partículas de carga incorporadas à matriz resinosa são polares, a matriz é essencialmente apolar. Esta característica dificulta a dispersão efetiva entre as duas fases. Desta forma, a utilização de agentes de união aumenta a adesão entre a matriz polimérica e a fase inorgânica levando a uma melhor transferência de cargas e maior resistência ao desgaste (Mohsen e Craig, 1995; Lim, Ferracane *et al.*, 2002).

Atualmente, os agentes de união mais utilizados na elaboração dos compósitos dentais são os organosilanos. Os silanos contêm grupos silânicos que podem aderir aos silanóis na superfície das partículas de carga e grupamentos metacrilato que se unem à resina, promovendo a união entre as fases orgânica e inorgânica (Debnath, Wunder *et al.*, 2003; Mitra, Wu *et al.*, 2003; Matinlinna, Lassila *et al.*, 2004; Wilson e Antonucci, 2006). Entretanto, tem sido demonstrado que a hidrólise pode quebrar a união entre o silano e as partículas de carga, o que seria uma das principais causas de falhas dos compósitos dentais, levando à formação de zonas de concentração de tensões e ao deslocamento de partículas (Soderholm e

Shang, 1993; Drummond, 2008). Outro problema da utilização do silano como agente de união é sua dependência à presença de sílica nas partículas de carga; sendo esta radiolúcida, tem sido substituída parcialmente por vidros contendo metais pesados nos compósitos dentais (Chan, Titus *et al.*, 1999; Amirouche-Korichi, Mouzali *et al.*, 2009).

Outros potenciais agentes de união, embora pouco estudados, são os monômeros ácidos funcionais. Estes são caracterizados pela presença de três diferentes segmentos: um grupo polimerizável, um espaçador de diferente natureza e comprimento, e uma terminação ácida (ácido carboxílico, fosfórico ou fosfônico) (Ogliari, Da Silva *et al.*, 2008). Estudos têm demonstrado que grupos funcionais capazes de liberar um ou mais prótons, como os grupos carboxil e fosfato, podem se unir a óxidos metálicos presentes nas partículas de carga dos compósitos por uma reação de quelação (Chan, Titus *et al.*, 1999; Behr, Rosentritt *et al.*, 2003; Masuno, Koizumi *et al.*, 2010). Esta propriedade dos grupos funcionais habilita os monômeros ácidos a serem utilizados como agentes de união entre a matriz resinosa e as partículas inorgânicas, embora esta capacidade não esteja completamente esclarecida.

1.2 JUSTIFICATIVA

Os cimentos resinosos são materiais amplamente utilizados na odontologia restauradora atual. Contudo, a formulação destes cimentos não está completamente desenvolvida e seu melhoramento afetará positivamente o resultado dos trabalhos clínicos realizados. Além disso, existe um apelo mercadológico muito intenso quanto à utilização de nanopartículas nos compósitos odontológicos, embora seus reais benefícios não estejam esclarecidos; e, à incorporação de cargas com diferentes composições, necessitando de diferentes agentes de união entre partículas, onde se enquadram os monômeros ácidos. Desta forma, estudos que busquem o aprimoramento e o entendimento da composição destes materiais então indicados.

1.3 OBJETIVOS

Preparar e testar cimentos resinosos experimentais com diferentes quantidades de nanopartículas e diferentes agentes de união entre a carga e a matriz resinosa.

Avaliar, isoladamente, o desempenho da incorporação de nanopartículas ao cimento resinoso e da utilização de monômeros ácidos como agentes de união entre as partículas de carga e a matriz resinosa, através da análise do grau de conversão, da resistência à flexão, do módulo de elasticidade, da microdureza, da espessura de película e da microscopia.

A hipótese nula a ser testada é que em cimentos resinosos a quantidade de nanopartículas e o tipo de agente de união aplicado às partículas não influenciam suas características e propriedades mecânicas.

1.4 MATERIAIS E MÉTODOS

1.4.1 Considerações iniciais

Este projeto será dividido em dois estudos executados concomitantemente: estudo do efeito da incorporação de nanopartículas ao cimento resinoso e estudo da influência da utilização de monômeros ácidos como agentes de união no tratamento de partículas de carga. A metodologia dos ensaios será a mesma para os dois estudos.

1.4.2 Preparo dos cimentos resinosos

1.4.2.1 Matriz resinosa modelo

Para os dois estudos será utilizada uma única matriz resinosa modelo composta por (concentração em massa): 50% de éster do bisfenol-A com dimetacrilato de glicidila (Bis-GMA, Esstech Inc., Essington, PA, EUA) e 50% de dimetacrilato de trietilenoglicol (TEGDMA, Esstech Inc.). Nesta resina será incorporado (concentração em massa): 0,4% de canforoquinona (Esstech Inc.) como fotoiniciador da polimerização, 0,8% de benzoato de etil 4-dimetilamino (Sigma-Aldrich, St. Louis, MO, EUA) como co-iniciador e 0,1% de hidroxitolueno butilado (Sigma-Aldrich) como inibidor. Os monômeros componentes da resina adesiva modelo serão misturados mecanicamente por 5min e levados à cuba ultrassônica (Plana CT CBU 100 / 1LDG, Tatuapé, SP, Brasil), por 10min, para homogeneização da mistura.

1.4.2.2 Confecção dos cimentos resinosos para estudo do efeito da incorporação de nanopartículas às partículas de carga

Cinco cimentos resinosos experimentais serão formulados através da incorporação de diferentes porcentagens de partículas de bário borosilicato de vidro silanizadas (Esstech Inc. – tamanho médio das partículas: 2µm) e de sílica coloidal (Aerosil 380; Degussa, Frankfurt, Alemanha – Tamanho médio das partículas: 7nm) na matriz resinosa modelo (Tab. 1).

A sílica coloidal será previamente silanizada por meio da imersão em solução de etanol absoluto (Synth, Diadema, SP, Brasil) com 5% de metacrilato de 3-trimetoxisilil propil (Sigma-Aldrich), em relação à massa de partículas. As partículas serão embebidas na solução e levadas à estufa (54°C por 24h), para assegurar a completa remoção do solvente. Após, as partículas serão passadas através de uma peneira de 150µm para desagregação.

Tabela 1. Porcentagem de partículas nos cimentos resinosos.

Grupo	Porcentagens de partículas (em massa)	
	Vidro de borosilicato de bário	Sílica coloidal
G1	60%	0%
G2	59%	1%
G3	57,5%	2,5%
G4	55%	5%
G5	50%	10%

As partículas de carga serão incorporadas à matriz através de intensa espatulação manual, seguida de espatulação mecânica (15min). O cimento será levado ao ultrasom (Plana CT CBU 100), por 1h, para homogeneização.

1.4.2.3 Confecção dos cimentos resinosos para estudo do efeito da utilização de monômeros ácidos como agentes de união entre as partículas de carga e a matriz resinosa

Para este estudo, micropartículas de vidro de Ba-B-Al-Si (Schott, Mainz, Alemanha), com tamanho médio de 3µm, e nanopartículas de sílica coloidal (Aerosil 380), com tamanho médio de 7nm, serão submetidas aos seguintes tratamentos de superfície (Tab. 2 / Fig. 1): cobertura com silano, cobertura com monômero ácido carboxilado e cobertura com monômero ácido fosforado. Um grupo será mantido sem tratamento das partículas para servir como controle negativo.

Tabela 2. Tratamentos de partículas utilizados no estudo.

Tratamento de partículas	Agente de união	Fabricante
Nenhum	-	-
Silano	metacrilato de 3-trimetoxisilil propil	Sigma-Aldrich
Monômero ácido carboxilado	maleato de mono-2 metacriloiloxietil	Sigma-Aldrich
Monômero ácido fosforado	Mistura equimolar de dihidrogênio fosfato de metacriloiloxietila / dihidrogênio fosfato de bis-metacriloiloxietila	CDC-Bio/UFPel

A quantidade de agente de união será de 5% (em massa) em relação à massa das partículas. O agente de união será diluído em etanol absoluto (Synth) e a esta solução serão incorporadas as partículas de carga. A solução será levada a 54°C, por 24h, para a completa remoção do solvente e, em seguida, as partículas serão passadas em uma peneira de 150µm para desaglomeração das partículas.

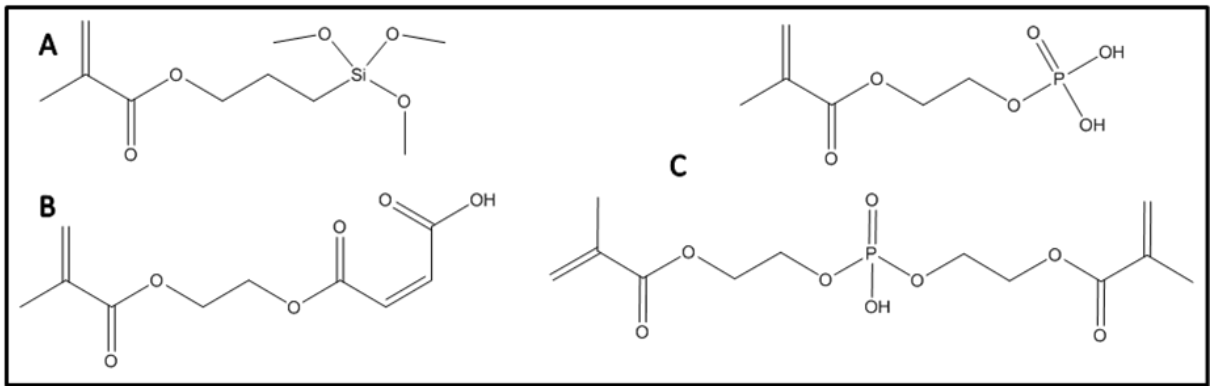

Figura 1. Estruturas moleculares: (A) metacrilato de 3-trimetoxisilil propil, (B) maleato de mono-2 metacriloiloxietil e (C) dihidrogênio fosfato de metacriloiloxietila / dihidrogênio fosfato de bis-metacriloiloxietila.

As partículas serão incorporadas em taxas de 59% de micropartículas e 1% de nanopartículas em relação à massa da matriz resinosa através de espatulação manual. Em seguida o cimento será submetido à espatulação mecânica (15min) e colocado em cuba de ultrassom (1h), para assegurar a adequada dispersão das partículas.

1.4.3 Análises dos cimentos resinosos

1.4.3.1 Cálculo de amostra

Este trabalho abrange materiais que serão elaborados especificamente para seu desenvolvimento. Desta forma, não existem dados na literatura que permitam embasamento científico para cálculo de amostra. Os números de repetições especificadas nas metodologias acima estão baseados em valores comumente utilizados na literatura e serão confirmados após a realização do ensaio piloto, buscando-se obter o poder do teste igual ou superior a 0,8.

1.4.3.2 Avaliação do grau de conversão

O grau de conversão será avaliado utilizando espectrofotômetro de infravermelho por transformada de Fourier (Prestige-21; Shimadzu, Tóquio, Japão) equipado com dispositivo de refletância total atenuada (ATR) apresentando um cristal horizontal de seleneto de zinco (Fig. 2). Um suporte será acoplado para fixação da unidade fotoativadora por diodo emissor de luz – LED (Radii; SDI, Bayswater, Victoria, Austrália) ao espectrômetro, permitindo a padronização de uma distância de 2mm entre a extremidade da ponteira e a amostra. A unidade fotoativadora será constantemente monitorada através de um radiômetro (Demetron Research Corporation, Danbury, CT, EUA) para obtenção de irradiância de 600 mW/cm^2.

As amostras serão dispensadas diretamente no cristal de seleneto de zinco, se restringindo ao tamanho do diâmetro da ponteira do LED, e imediatamente será feita a primeira leitura (monômero). Após a amostra ser fotoativada por 40s, uma segunda leitura será feita (polímero). Cada cimento resinoso será avaliado cinco vezes.

O grau de conversão será calculado considerando a intensidade da vibração do tipo estiramento da dupla ligação carbono-carbono na freqüência de $1635cm^{-1}$. O estiramento simétrico do anel aromático em $1610cm^{-1}$ das amostras polimerizadas e não-polimerizadas será utilizado como padrão interno. As leituras serão feitas conforme as seguintes condições: 32 escaneamentos, resolução $4cm^{-1}$, apodização de Happ-Genzel e velocidade do deslocamento do espelho de 2,8mm/s. A análise será realizada em ambiente com temperatura controlada de 23ºC e umidade relativa menor que 60%.

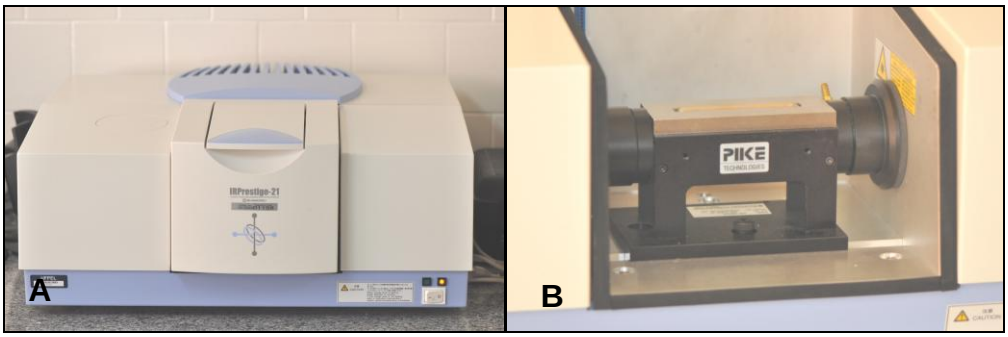

Figura 2. Espectrofotômetro de infravermelho por transformada de Fourier Shimadzu, Prestige 21 (A), dispositivo de ATR (B).

1.4.3.3 Ensaio de resistência à mini-flexão e módulo de elasticidade

Serão confeccionados 20 corpos de prova por cimento resinoso com auxílio de uma matriz metálica bipartida (dimensão interna 10 × 2 × 2mm) posicionada sobre uma tira de poliéster e encaixada em uma base metálica. Os cimentos resinosos serão dispensados no interior da matriz e recobertos com outra tira de poliéster. Para fotoativação dos corpos de prova será utilizado o aparelho fotopolimerizador LED (Radii), em duas janelas de 40s de exposição em cada lado do espécime. Os palitos obtidos terão os excessos removidos e as laterais serão polidas com auxílio de lixas de carboneto de silício, granulação 600 e 1200 e serão armazenados protegidos da luz, a 37°C, por 24h.

Os palitos terão sua largura e espessura mensuradas utilizando um paquímetro digital (Mitutoyo, Suzano, SP, Brasil), com precisão de 0,01mm, para o cálculo da área de cada espécime. Os corpos de prova serão submetidos ao teste de resistência flexural de três pontos em uma máquina de ensaios mecânicos (Emic, DL 500, São José dos Pinhais, PR, Brasil), com velocidade de 0,5mm/min e distância entre os pontos de 8mm, até sua falha (Fig. 3). A resistência à flexão (σ) será calculada em megapascal (MPa) de acordo com a equação:

$$\sigma = 3Fl/ 2bh^2$$

onde F é a força máxima (N), l é a distância (mm) entre os suportes, b é a largura (mm) e h é a altura (mm) do espécime imediatamente antes do teste.

O módulo de elasticidade será calculado pela relação entre os valores da tensão e da deformação linear específica, na fase elástica. A expressão matemática usada para o cálculo desta constante é:

$$E = T/ \varepsilon$$

onde E é o módulo de elasticidade (GPa), T é a tensão aplicada (MPa) e ε a deformação linear específica (mm).

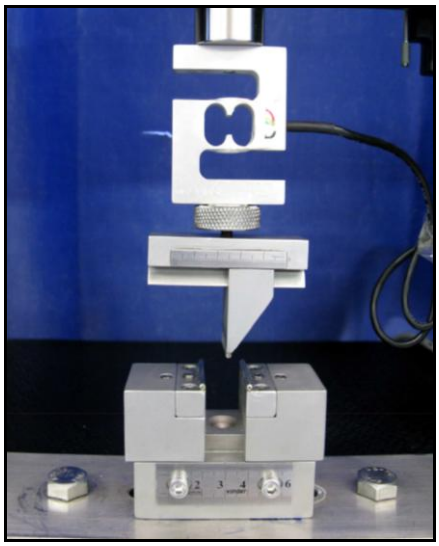

Figura 3. Máquina de Ensaios Universal EMIC DL500 com dispositivo adaptado para ensaio de miniflexão.

1.4.3.4 Avaliação da microdureza

Para avaliação da microdureza cinco corpos-de-prova por cimento serão confeccionados com o auxílio de uma matriz metálica circular (5mm de diâmetro x 2mm de altura), recoberta em ambos os lados com uma tira de poliéster. O cimento resinoso será dispensado na matriz e fotoativado (LED) por 40 segundos de cada lado. Após serem armazenados protegidos da luz (24h, a 37°C), os espécimes serão submetidos a acabamento com lixas de granulação decrescente (800, 1000, 1200 e

1500) com auxílio de uma politriz metalográfica (Aropol - E, Arotec S.A. Indústria e Comércio, Cotia, SP, Brasil).

O ensaio de dureza Knoop será realizado em um microdurômetro (Futuretech FM 700, Tóquio, Japão) com procedimento automático de aplicação de 25g de carga durante 5 segundos (Fig. 4). As mensurações de microdureza serão realizadas mediante aumento de 500x. Para cada corpo-de-prova serão feitas três endentações e calculada uma média de microdureza Knoop.

Figura 4. Durômetro Futuretech FM700

1.4.3.5 Avaliação da espessura de película

Para avaliar a espessura de película serão utilizadas duas lâminas de vidro com cinco milímetros de espessura e uma área de superfície de 200mm^2. A espessura combinada das duas lâminas de vidro será mensurada (leitura A) com um micrômetro digital (MDC-Lite; Mitutoyo, Suzano, SP, Brasil), com precisão de 0,01mm. Posteriormente, 0,1mL de cimento resinoso será colocado numa posição central entre as placas e uma carga constante de 150N será cuidadosamente aplicada sobre a placa superior, por 180s (Fig. 5). Após este período, o cimento será submetido à irradiação com LED (40s) para estabilizar os espécimes. Uma segunda leitura será executada com as lâminas de vidro unidas pelo cimento resinoso (leitura B). A espessura de película será calculada com a subtração dos valores obtidos na leitura A dos valores obtidos na leitura B. Cinco mensurações serão realizadas por cimento resinoso.

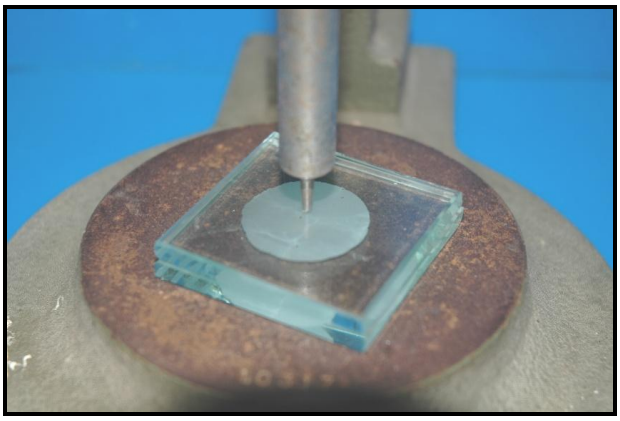

Figura 5. Compressão das placas com 150N.

1.4.3.6 Análise em microscopia

Para observar a dispersão e a interação entre as partículas de carga e a matriz resinosa, os espécimes utilizados para a avaliação da microdureza serão embutidos em resina epóxica e submetidos a acabamento com lixas de granulação decrescente (800, 1000, 1200 e 1500) e polimento com pastas diamantadas de granulação decrescente (3, 1, 0,25, e 0,1µm), com auxílio de uma politriz metalográfica (Aropol). A seguir, serão recobertos com ouro e examinados com microscópio eletrônico de varredura (SSX-550; Shimadzu), Fig. 6.

Figura 6. Microscópio eletrônico de varredura.

1.4.4 Análise estatística

O método estatístico mais apropriado será escolhido com base na aderência ao modelo de distribuição normal e igualdade de variância, será utilizado o programa estatístico SigmaStat 3.01 (Systat INC, Chicago, IL, EUA). Para todos os testes será considerado o valor $p<0,05$ como estatisticamente significante.

1.5 REFERÊNCIAS

Amirouche-Korichi, A., M. Mouzali*, et al.* Effects of monomer ratios and highly radiopaque fillers on degree of conversion and shrinkage-strain of dental resin composites. **Dental Materials**, v.25, n.11, Nov, p.1411-8. 2009.

Behr, M., M. Rosentritt*, et al.* Adhesive bond of veneering composites on various metal surfaces using silicoating, titanium-coating or functional monomers. **Journal of Dentistry** , v.31, n.1, Jan, p.33-42. 2003.

Chan, D. C., H. W. Titus*, et al.* Radiopacity of tantalum oxide nanoparticle filled resins. **Dental Materials**, v.15, n.3, May, p.219-22. 1999.

Debnath, S., S. L. Wunder*, et al.* Silane treatment effects on glass/resin interfacial shear strengths. **Dental Materials**, v.19, n.5, Jul, p.441-8. 2003.

Drummond, J. L. Degradation, fatigue, and failure of resin dental composite materials. **Journal of Dental Research** , v.87, n.8, Aug, p.710-9. 2008.

Habekost, L. V., G. B. Camacho*, et al.* Tensile bond strength and flexural modulus of resin cements--influence on the fracture resistance of teeth restored with ceramic inlays. **Operative Dentistry**, v.32, n.5, Sep-Oct, p.488-95. 2007.

Ikejima, I., R. Nomoto*, et al.* Shear punch strength and flexural strength of model composites with varying filler volume fraction, particle size and silanation. **Dental Materials**, v.19, n.3, May, p.206-11. 2003.

Kim, J. W., L. U. Kim*, et al.* Size control of silica nanoparticles and their surface treatment for fabrication of dental nanocomposites. **Biomacromolecules**, v.8, n.1, Jan, p.215-22. 2007.

Lim, B. S., J. L. Ferracane*, et al.* Effect of filler fraction and filler surface treatment on wear of microfilled composites. **Dental Materials**, v.18, n.1, Jan, p.1-11. 2002.

Lin, C. T., S. Y. Lee*, et al.* Influence of silanization and filler fraction on aged dental composites. **Journal of Oral Rehabilitation**, v.27, n.11, Nov, p.919-26. 2000.

Masuno, T., H. Koizumi*, et al.* Effect of Acidic Monomers on Bonding to SUS XM27 Stainless Steel, Iron, and Chromium with a Tri-n-butylborane-initiated Acrylic Resin. **The Journal of Adhesive Dentistry** , Feb 12. 2010.

Matinlinna, J. P., L. V. Lassila*, et al.* An introduction to silanes and their clinical applications in dentistry. **Int J Prosthodont**, v.17, n.2, Mar-Apr, p.155-64. 2004.

Mitra, S. B., D. Wu*, et al.* An application of nanotechnology in advanced dental materials. **J Am Dent Assoc**, v.134, n.10, Oct, p.1382-90. 2003.

Mohsen, N. M. e R. G. Craig. Effect of silanation of fillers on their dispersability by monomer systems. **Journal of Oral Rehabilitation**, v.22, n.3, Mar, p.183-9. 1995.

Ogliari, F. A., E. O. Da Silva*, et al.* Synthesis of phosphate monomers and bonding to dentin: esterification methods and use of phosphorus pentoxide. **Journal of Dentistry** , v.36, n.3, Mar, p.171-7. 2008.

Soderholm, K. J. e S. W. Shang. Molecular orientation of silane at the surface of colloidal silica. **Journal of Dental Research** , v.72, n.6, Jun, p.1050-4. 1993.

Tian, M., Y. Gao*, et al.* Fabrication and evaluation of Bis-GMA/TEGDMA dental resins/composites containing nano fibrillar silicate. **Dental Materials**, v.24, n.2, Feb, p.235-43. 2008.

Wilson, K. S. e J. M. Antonucci. Interphase structure-property relationships in thermoset dimethacrylate nanocomposites. **Dental Materials**, v.22, n.11, Nov, p.995-1001. 2006.

Wilson, K. S., K. Zhang*, et al.* Systematic variation of interfacial phase reactivity in dental nanocomposites. **Biomaterials**, v.26, n.25, Sep, p.5095-103. 2005.

1.6 ORÇAMENTO

Quadro 1. Orçamento previsto para a viabilização do projeto.

Descrição	**Quantidade**	**Valor R$**
Metacrilato de 3-trimetoxisilil propil metacrilato	100mL	480,00
Vidro de borosilicato de bário	100g	450,00
Éster do bisfenol-A com dimetacrilato de glicidila	500g	188,00
Canforoquinona	25g	410,00
Etanol	500mL	19,48
Benzoato de etil 4-dimetilamino	100g	300,00
Folhas A4	2 pacotes	30,00
Hidroxitolueno butilado	25g	410,00
Impressão da tese	5 unidades	250,00
Lixas metalográficas	30 unidades	45,00
Micropartículas de vidro de Ba-B-Al-Si	100g	360,00
Maleato de mono-2 metacriloiloxietil	100mL	210,00
Nitrogênio liquido	10L	70,00
Resina epóxica	1 kit	50,00
Serviço de revisão do Inglês	2	250,00
Sílica coloidal	50g	350,00
Toner impressora	1unidade	150,00
Dimetacrilato de trietilenoglicol	250mL	197,00
Utilização do microscópio eletrônico	8h	400,00
TOTAL	____	5.259,48

1.7 CRONOGRAMA

Quadro 2. Cronograma previsto de atividades.

Ano	Mês	Revisão de literatura	Ensaios Laboratoriais	Redação dos artigos	Submissão dos artigos	Conclusão
2008	Junho	X	X			
	Julho	X	X			
	Agosto	X	X			
	Setembro	X	X			
	Outubro	X	X			
	Novembro	X	X			
	Dezembro	X	X			
2009	Janeiro	X				
	Fevereiro	X				
	Março	X				
	Abril	X				
	Maio	X		X		
	Junho	X		X		
	Julho	X				
	Agosto	X				
	Setembro	X	X			
	Outubro	X	X			
	Novembro	X	X			
	Dezembro	X	X			
2010	Janeiro	X	X			
	Fevereiro	X	X			
	Março	X		X		
	Abril	X		X		
	Maio	X	X			
	Junho	X		X		
	Julho	X		X		Qualificação
	Agosto			X		
	Setembro				X	Defesa

1.8 ORGANOGRAMAS DO PROJETO

Correspondente ao Artigo 1.

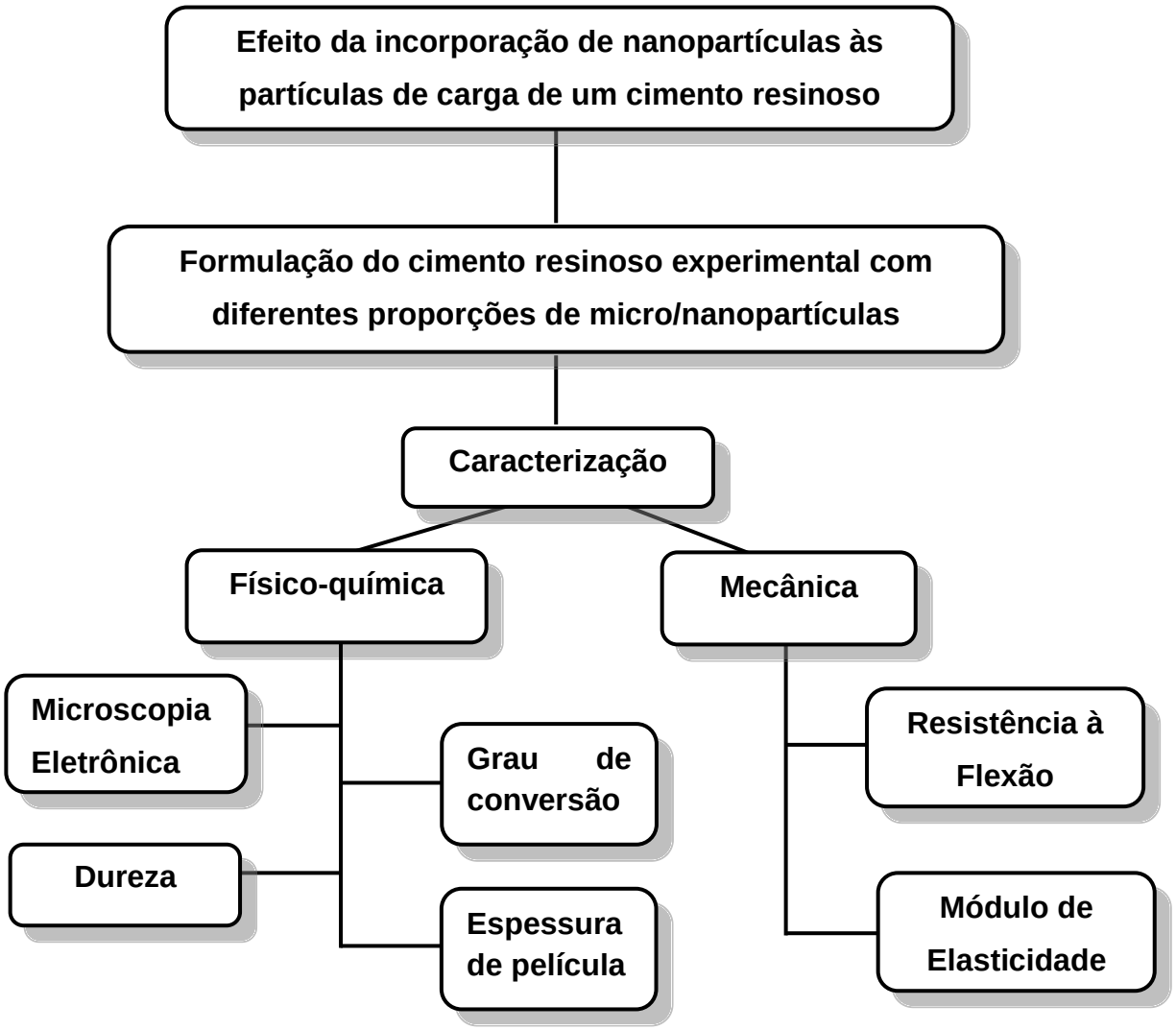

Correspondente ao Artigo 2.

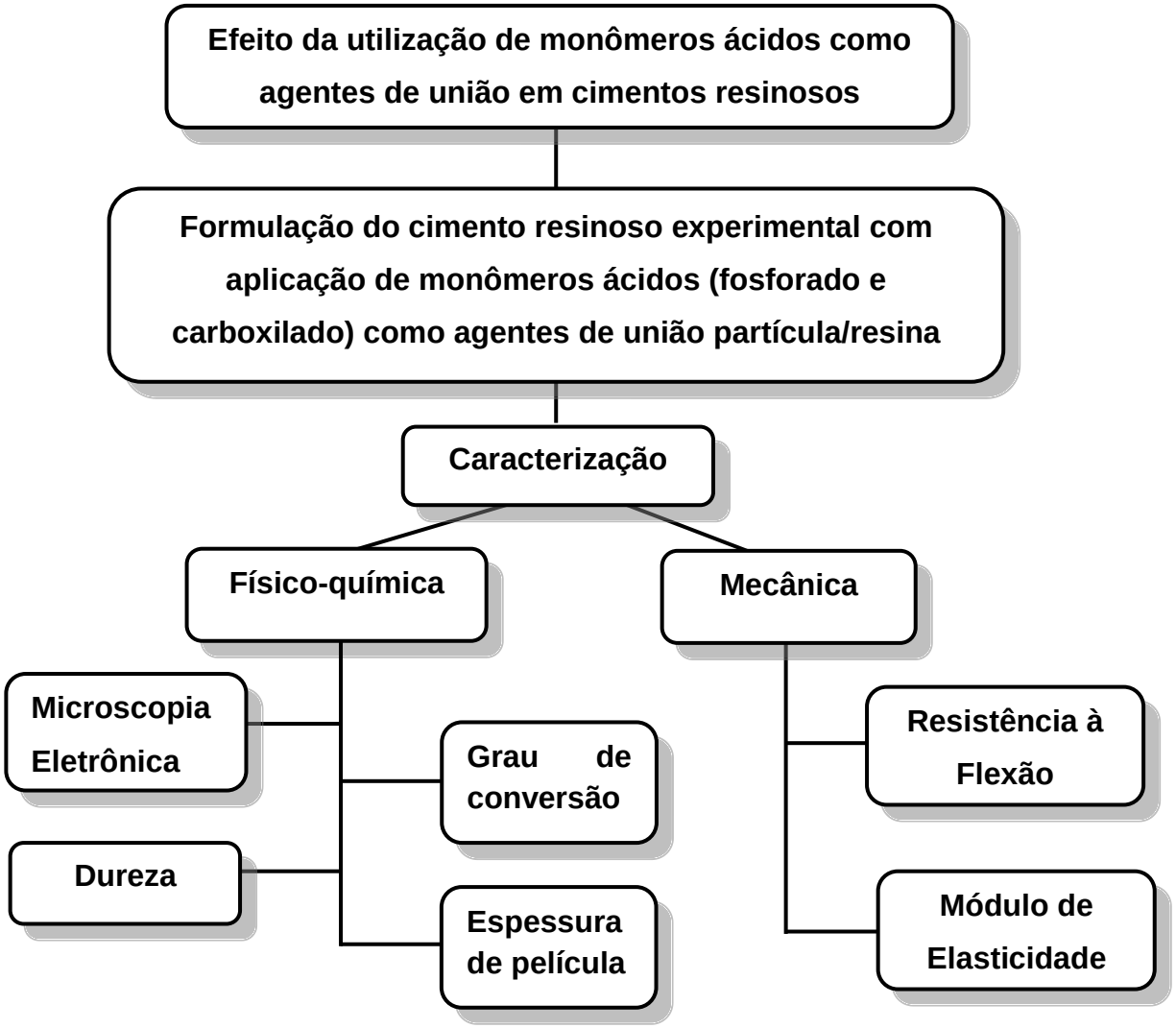

Nota: Os dois artigos serão submetidos ao periódico Journal of Dentistry

2 ARTIGO 1* - Influence of nanoparticle loading on properties of particulate hybrid resin luting agents

* Artigo redigido segundo o Guia para Autores do Periódico Journal of Applied Polymer Science, disponível em:
http://onlinelibrary.wiley.com/journal/10.1002/(ISSN)1097-4628/homepage/ForAuthors.html
Acesso em: 17 de dezembro de 2010.

Influence of nanoparticle loading on properties of particulate hybrid resin luting agents

Luciano V. Habekost[a], Guilherme B. Camacho[a], Giana S. Lima[a], Fabrício A. Ogliari[b], Glória B. Cubas[a], Rafael R. Moraes[a]

[a]School of Dentistry, Federal University of Pelotas;
R. Gonçalves Chaves 457, 96015-560, Pelotas-RS, Brazil

[b]Materials Engineering School, Federal University of Pelotas;
R. Félix da Cunha 809, 96010-000, Pelotas-RS, Brazil

Corresponding author:
Prof. Rafael R. Moraes
School of Dentistry, Federal University of Pelotas
R. Gonçalves Chaves 457, 96015-560, Pelotas-RS, Brazil
Telephone/Fax: 55 53 3222.6690 (moraesrr@gmail.com)

Influence of nanoparticle loading on properties of particulate hybrid resin luting agents

Keywords: filler; mechanical properties; nanoparticle; resin luting agents; SEM.

Abstract

This study investigated the influence of nanoparticle loading on properties of hybrid resin luting agents. Silanated 2-µm barium borosilicate glass microparticles and 7-nm silica nanoparticles were used. Five luting agents were obtained by loading a photo-curable Bis-GMA:TEGDMA co-monomer with a total mass faction of 60% of inorganic fillers; the mass fraction of nanoparticles was set at 0 (control), 1 (G1), 2.5 (G2.5), 5 (G5) or 10% (G10). The properties evaluated were flexural strength (σ) and modulus (E_f), Knoop hardness number (KHN), and film thickness (FT). Dispersion/interaction of the particles with the resin phase was assessed by scanning electron microscopy (SEM). Data were submitted to statistical analysis (5%). For σ, G1 > G2.5 = G5 = G10, and control > G10. For E_f, G2.5 > control = G1 > G5 > G10. For KHN, G5 = G10 > control = G1 = G2.5. For FT, G10 = G5 > control = G1, and G10 > G2.5. Incorporation of nanoparticles was associated with observation of clusters in the SEM analysis. The clusters were more frequent for higher nanoparticle loadings. Moderate incorporation of nanoparticles may improve the properties of resin luting agents. Mass fractions above 2.5% may present detrimental effects on the properties.

Introdution

The use of resin luting agents to lute ceramic restorations has been associated with a strengthening effect of the restorative;[1,2] the higher the mechanical properties of the luting agent, the higher the fracture resistance of the luted ceramic.[2,3] Dental resin luting agents consist of a resin matrix reinforced with inorganic particles; a coupling agent mediates the bond between these two phases. The introduction of well-dispersed inorganic particles into the resin phase has been shown to greatly influence the performance of polymer composites.[4] The dispersed phase is designed to enhance the modulus of the softer polymer phase and usually consists of glass or ceramic particles of different compositions and sizes.

Nanostructured dental composites were introduced in an endeavor to enhance their esthetic properties by increasing the retention of polish and gloss while having equivalent or improved physical properties compared with traditional hybrid composites.[5] It is known that the shape, amount and size of the particles reinforcing the composite might affect its properties. Decreasing the interparticle space is a key to improve the mechanical strength by increasing the protection of the softer resin matrix. Reduced interparticle spacing may be achieved by either decreasing the size of the particles or increasing the volume fraction of fillers.[6,7] The advantage of hybrid materials is that the introduction of nanoparticles may fill the areas between larger microparticles, allowing for accommodation of higher filler levels without drastically interfering with the handling properties of the composite.

Due to their small size and high surface area, nanoparticles have been also associated the formation of clusters within the mixed composite.[8] Depending on the connective status of the fillers within the clusters, these may either increase the mechanical properties or act as stress-concentrating areas, decreasing the polymer strength.[9] Therefore, the literature presents contrasting results regarding the properties of composites modified with nanoparticles; these have shown either similar,[10-12] slightly better[10] or worse results[12,13] compared with traditional hybrid materials. The effect of nanoparticle incorporation into resin luting agents, however, is still unknown.

The aim of this study was to investigate the influence of the nanoparticle fraction incorporated to dental hybrid resin luting agents on key properties of these

materials. The null-hypotheses tested were: (I) the properties of the resin luting agents would be independent of the nanoparticle fraction; and (II) there would be no differences in the ultrastructural features of luting agents obtained with different nanoparticle fractions.

Material and Methods

Formulation of the resin luting agents

A model dimethacrylate comonomer blend based on a 1:1 mass ratio of 2,2-bis[4-(2-hydroxy-3-methacryloxypropoxy)phenyl]propane (Bis-GMA) and triethyleneglycol dimethacrylate (TEGDMA) (Esstech Inc., Essington, PA, USA) was loaded with a 0.4% mass fraction of camphorquinone (Esstech), 0.8% mass fraction of ethyl 4-dimethylamino benzoate (Sigma-Aldrich, St. Louis, MO, USA), and 0.1% mass fraction of butylated hydroxytoluene (Sigma-Aldrich) as radical scavenger. All chemicals were used as received.

Barium borosilicate glass microparticles 2 μm average size (Esstech) and silica nanoparticles 7 nm average size (Aerosil 380; Degussa, Germany) were coated with 5 wt% of the silane coupling agent 3-(trimethoxysilyl)propyl methacrylate (Sigma-Aldrich). The silane was diluted in ethanol, the particles soaked into the solution and left to dry at 54°C for 24 h to assure complete solvent removal. After storage, the fillers were sieved through a 150-μm sieve. Five resin luting agents were obtained by loading the model blend with a mass faction of 60% of inorganic fillers. From the total mass of 60%, the mass fraction of nanoparticles was set at 0 (control), 1, 2.5, 5 or 10%. The particles were incorporated by intensive manual mixing followed by mechanical stirring with a motorized mixer. In order to assure the adequate dispersion of the filler system, the materials were ultrasonicated for 1 h.

Flexural strength and modulus

Flexural tests were performed using eighteen bar specimens with dimensions of 12 × 2 × 2 mm (8 mm span width). The resin luting agent was placed into the

stainless steel/glass mold, covered with a Mylar strip and photoactivated using two irradiations of 40 s on each side. 24 h after irradiation, a three-point bending test was carried out on a mechanical testing machine (DL500; EMIC, São José dos Pinhais, PR, Brazil) at a crosshead speed of 0.5 mm/min. Flexural strength (σ) and flexural modulus (E_f) were calculated from the load-displacement trace.

Hardness

The materials were placed into cylinder-shaped metal molds (5 mm inner diameter × 2 mm thick), covered with a Mylar strip and photoactivated for 40 s on each surface. After 24 h, the specimens were wet-ground with 800-, 1000-, 1200- and 1500-grit SiC abrasive papers. Three readings were performed on each specimen through a microindenter (FM-700; Future-Tech, Kawasaki, Japan), under a load of 25 g and a dwell time of 5 s. The Knoop hardness number (KHN, kgf/mm^2) for each specimen was recorded as the average of the three indentations. Five specimens were tested for each luting agent.

Film thickness

Two optically flat square glass plates, each 5 mm thick, and having a contact surface area of 200 mm^2 were used. The combined thickness of the glass plates stacked in contact was measured (reading A) with a digital caliper (MDC-Lite; Mitutoyo, Suzano, SP, Brazil), accurate to 0.001 mm. Then, 0.1 mL of resin luting agent was placed centrally between the plates, and a constant load of 150 N was carefully applied vertically and centrally via the top plate, for 180 s. After this period, light irradiation was performed for 40 s in order to stabilize the specimen. The combined thickness of the two glass plates and the luting agent film was measured (reading B). Film thickness was recorded as the difference between reading B and reading A. Five specimens were tested for each luting agent.

SEM analysis

In order to observe the dispersion and interaction of the filler particles within the resin phase, cylinder-shaped specimens (5 mm diameter × 1 mm thick) were embedded in epoxy resin and wet-polished with 600-, 1200-, 1500-, 2000- and 2500-grit SiC papers and with 3, 1, 0.25 and 0.1 μm diamond polishing suspensions. The specimens were coated with gold and the polished surfaces examined by scanning electron microscopy – SEM (SSX-550; Shimadzu) at 15 kV.

Statistical analysis

Data for flexural strength, hardness and film thickness were submitted to one-way ANOVA. Elastic modulus data did not achieve the homocedasticity criteria and was submitted to ANOVA on Ranks. All pairwise multiple comparison procedures were carried out by the Student-Newman-Keuls' method. Regression analyses were used to investigate the relationship between the gradual addition of nanoparticles and each property. The 0.05 significance level was set for all analyses.

Results

Results for all evaluations are shown in Table 1. Non-linear regression plots are shown in Figure 1. The material with 1% of nanoparticles showed significantly higher flexural strength than luting agents with 2.5, 5 and 10% of nanoparticles ($P \leq 0.046$). The control luting agent showed significantly higher flexural strength as compared with the material 10% of nanoparticles ($P = 0.049$). The regression model for flexural strength showed a peak behavior ($R^2 = 0.997$), although it was not significant ($P = 0.329$). The luting agent with 2.5% of nanoparticles showed significantly higher flexural modulus compared with all the other luting agents ($P < 0.05$); similar results were observed for the luting agents with 0 and 1% of nanoparticles ($P > 0.05$), both showing significantly higher modulus than the luting agent with 5% of nanoparticles ($P < 0.05$). The material with 10% of nanoparticles showed significantly lower modulus than all the other luting agents ($P < 0.05$). The regression curve followed a rational behavior ($R^2 = 0.578$), but the model was not statistically significant ($P = 0.084$).

Hardness of the luting agents with 5 and 10% of nanoparticles was significantly higher compared with all the other luting agents ($P \leq 0.031$). Materials with 0, 1 and 2.5% of nanoparticles showed similar hardness ($P \geq 0.389$). The regression curve followed a sigmoidal behavior ($R^2 = 0.925$), but the model was not statistically significant ($P = 0.174$). For film thickness, materials with 0 and 1% of nanoparticles showed significantly lower values compared with the luting agents with 5 and 10% ($P \leq 0.048$), whereas the luting agent containing 2.5% of nanoparticles showed significantly lower value compared with the luting agent with 10% ($P \leq 0.05$). The regression model followed a linear significant behavior ($R^2 = 0.966$; $P < 0.01$), showing an increase in film thickness associated with the increase in the fraction of nanoparticles incorporated into the luting agent.

Representative SEM images of the luting agent surfaces are shown in Figure 2. The incorporation of nanoparticles was associated with the observation of nanoparticle clusters, which showed as darker areas surrounded by microparticles (examples are indicated by asterisks in Figures 2B to 2E). No clustering was detected in the control luting agent (Figure 2A). The clusters were more frequently observed for materials with higher nanoparticle loads.

Discussion

The first null-hypothesis was rejected because the nanoparticle fraction had a significant influence on the properties of the resin luting agents. Incorporation of 1% of nanoparticles increased the flexural strength, whereas dispersion of up to 2.5% of nanoparticles improved the flexural modulus. Beyond 2.5%, the incorporation of nanoparticles affected the flexural properties negatively. This result is in line with those from Tian et al.,[14] who investigated composites modified with nanofibrilar silicates. This drop in mechanical properties is likely a result of the possible reinforcement due to higher nanoparticle loading being offset by particle entanglement and agglomeration, which were observed in the SEM analysis. Therefore, the second null-hypothesis was also rejected. The spherical shape of nanoparticles should have advantages over irregular-shaped fillers regarding particle dispersion. Because spherical particles have only one point of contact, the tendency to agglomerate would be reduced, as a small surface area is available for

particle-particle attraction, and less energy is needed to break these interactions. However, this effect probably occurs for fillers with same particle size differing only in morphology, which is not the case here.

Large mass fractions of nanoparticles mixed into hybrid composites have been associated with impairment of the mechanical properties and formation of filler agglomerates in resin-based composites.[14] The presence of large clusters formed by small particles is also observed in commercial nanostructured restoratives.[10] The main point regarding the clusters is the connective status of the nanoparticles. Under stress loading, the connectivity between the fillers and of the fillers with the polymer matrix is critical, as a good link may halt the crack propagation in the matrix surrounding the fillers.[15] The interparticle spaces are very small inside the clusters; provided that strong connective forces between the nanoparticles themselves and the nanoparticles with the resin are obtained, these areas may have a protective effect in the structure. Poor connective forces, on the other hand, may lead the clusters to act as spots of stress concentration within the luting agent, impairing its mechanical properties.

The results for hardness followed another direction than did the flexural properties, as the incorporation of large fractions of nanoparticles increased the hardness values. It has been shown that hardness and flexural data may not correlate well for resin luting agents.[16] High nanoparticle loads quickly saturate the resin phase because nanoparticles have higher surface area than microparticles. Therefore, the surface of the composites occupied by fillers instead of the softer polymer phase is increased, leading to an increase in hardness.[17-19] This is a positive effect of nanoparticle incorporation into resin luting agents, as higher hardness values could be associated with increased wear resistance of the resin-based materials.[20]

The film thickness also increased as the incorporation of nanoparticles was incremented. An exponential increase in viscosity is associated with the increase in filler load; for identical filler fractions, the viscosity of the composite increases as the filler size decreases.[21] Due to the small particle size, the specific surface area of nanoparticles increases dramatically; therefore, more monomers are necessary to wet the surface of the particles. In addition to the resin-particle interaction, as the

filler load is increased or the filler size is reduced, there is an increase in the particle-particle interaction, decreasing the flow capacity of the luting agent. This might have a critical influence on the resulting thickness of the luting agent layer in the clinical situations. It is important to highlight, however, that all luting agent films were below the 50-µm value stated as limit for dental luting agents by the ISO 4049 specification.[22]

The present results show that the judicious incorporation of silanated silica nanoparticles may improve the properties of hybrid resin luting agents. Under loading, nanoparticles may have the ability to reorient in a stress dissipation mechanism in order to inhibit crack extension in semi-crystalline and amorphous polymers.[23,24] For surface coating polymers, crack healing mechanisms have been described, in which nanoparticles are attracted to the substrate, filling surface defects.[25] However, mass fractions above 2.5% should be avoided, as a detrimental effect on the properties becomes evident. The present results also show the incorporation of nanoparticles leads to formation of clusters within the mixed luting agent. This is corroborated by Tian et al.,[14] who have reported that it was still a challenge to achieve high degree of separation and uniform dispersion of silanized nanofibrilar silicates in a Bis-GMA/TEGDMA co-monomer.

References

1. G. J. Fleming, F. R. Maguire, G. Bhamra, F. M. Burkeand, P. M. Marquis. *J Dent Res*, **85**, 272-276 (2006).

2. O. Addison, P. M. Marquisand, G. J. Fleming. *J Dent Res*, **86**, 519-523 (2007).

3. L. V. Habekost, G. B. Camacho, F. F. Demarco, J. M. Powers. *Oper Dent*, **32**, 488-495 (2007).

4. M. H. Chen. *J Dent Res*, **89**, 549-560 (2010).

5. S. B. Mitra, D. Wuand, B. N. Holmes. *J Am Dent Assoc*, **134**, 1382-1390 (2003).

6. K. D. Jorgensen, P. Horsted, O. Janum, J. Kroghand, J. Schultz. *Scand J Dent Res*, **87**, 140-145 (1979).

7. B. S. Lim, J. L. Ferracane, J. R. Condonand, J. D. Adey. *Dent Mater*, **18**, 1-11 (2002).

8. K. S. Wilson, K. Zhangand, J. M. Antonucci. *Biomaterials*, **26**, 5095-5103 (2005).

9. J. L. Drummond. *J Dent Res*, **87**, 710-719 (2008).

10. R. R. Moraes, S. Goncalves L de, A. C. Lancellotti, S. Consani, L. Correr-Sobrinhoand, M. A. Sinhoreti. *Oper Dent*, **34**, 551-557 (2009).

11. Z. D. Yesil, S. Alapati, W. Johnstonand, R. R. Seghi. *J Prosthet Dent*, **99**, 435-443 (2008).

12. C. P. Turssi, J. L. Ferracaneand, L. L. Ferracane. *J Biomed Mater Res B Appl Biomater*, **78**, 196-203 (2006).

13. A. R. Curtis, W. M. Palin, G. J. Fleming, A. C. Shortalland, P. M. Marquis. *Dent Mater*, **25**, 188-197 (2009).

14. M. Tian, Y. Gao, Y. Liu, Y. Liao, N. E. Hedinand, H. Fong. *Dent Mater*, **24**, 235-243 (2008).

15. C. T. Lin, S. Y. Lee, E. S. Keh, D. R. Dong, H. M. Huangand, Y. H. Shih. *J Oral Rehabil*, **27**, 919-926 (2000).

16. R. R. Braga, P. F. Cesarand, C. C. Gonzaga. *J Oral Rehabil*, **29**, 257-262 (2002).

17. K. H. Chungand, E. H. Greener. *J Oral Rehabil*, **17**, 487-494 (1990).

18. M. Hosseinalipour, J. Javadpour, H. Rezaie, T. Dadrasand, A. N. Hayati. *J Prosthodont*, **19**, 112-117 (2010).

19. K. H. Kim, J. L. Ongand, O. Okuno. *J Prosthet Dent*, **87**, 642-649 (2002).

20. A. C. Faria, U. M. Benassi, R. C. Rodrigues, R. F. Ribeiroand, G. Mattos Mda. *Braz Dent J*, **18**, 60-64 (2007).

21. J. H. Lee, C. M. Umand, I. B. Lee. *Dent Mater*, **22**, 515-526 (2006).

22. *International Standard ISO 4049: Dentistry — Polymer-based restorative materials*, 5 (2009).

23. J. Y. Lee, Q. L. Zhang, T. Emrickand, A. J. Crosby. *Macromolecules*, **39**, 7392-7396 (2006).

24. D. Shah, P. Maiti, D. D. Jiang, C. A. Battand, E. P. Giannelis. *Advanced Materials*, **17**, 525-528 (2005).

25. K. A. Smith, S. Tyagiand, A. C. Balazs. *Macromolecules*, **38**, 10138-10147 (2005).

Table

Table 1. Means (SD) for flexural strength (σ), flexural modulus (E_f), hardness (KHN) and film thickness (FT)

	Nanoparticle loading (mass fraction)*				
	0%	1%	2,5%	5%	10%
σ, MPa	144 (18) ^{AB}	153 (9) ^{A}	140 (21) ^{BC}	132 (14) ^{BC}	131 (13) ^{C}
E_f, GPa	1.90 (0.4) ^{B}	1.85 (0.1) ^{B}	2.00 (0.2) ^{A}	1.77 (0.2) ^{C}	1.62 (0.1) ^{D}
KHN, kgf/mm^2	35.4 (1.7) ^{B}	37.7 (4.2) ^{B}	35.9 (2.2) ^{B}	44.2 (4.2) ^{A}	42.6 (3.6) ^{A}
FT, μm	25.2 (8.6) ^{C}	26.4 (8.1) ^{C}	33.0 (10.7) ^{BC}	39.8 (5.5) ^{AB}	48.8 (7.2) ^{A}

*The total mass fraction of inorganic fillers (nano and microparticles) was 60%.

Distinct letters in a same row indicate significant differences for nanoparticle loading ($P < 0.05$).

Figure Legends

Figure 1. Nonlinear regression plots used to investigate the relationship between the gradual addition of nanoparticles and each property.

Figure 2. Representative SEM images of polished luting agent surfaces with different nanoparticle loadings: (A) 0%; (B) 1%; (C) 2,5%; (D) 5%; (E) 10%. The incorporation of nanoparticles was associated with the observation of nanoparticle clusters (darker areas surrounded by microparticles, as indicated by asterisks in B to E). No clustering was detected in the control luting agent (A). The clusters were more frequently observed for materials with higher nanoparticle loading levels.

Figures

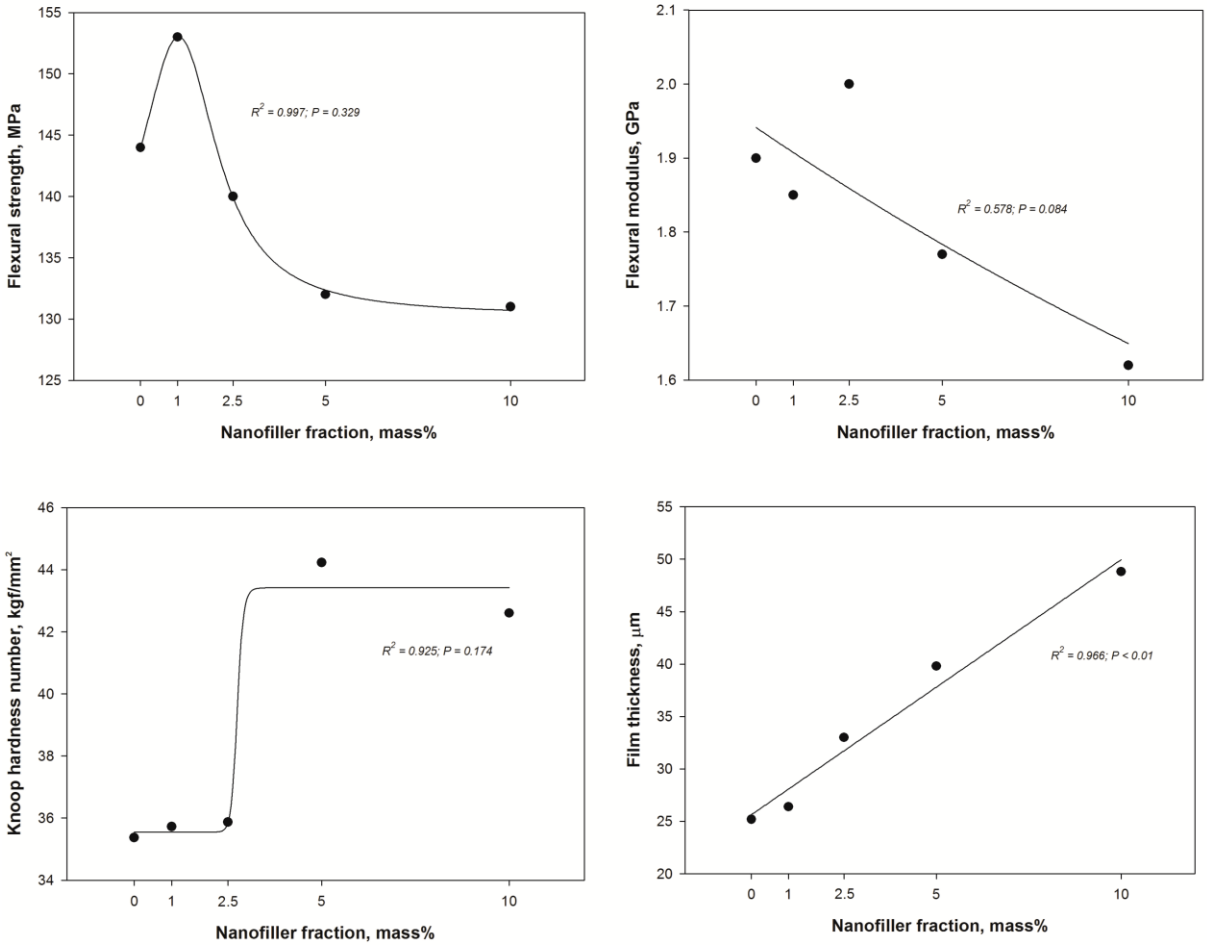

Figure 1

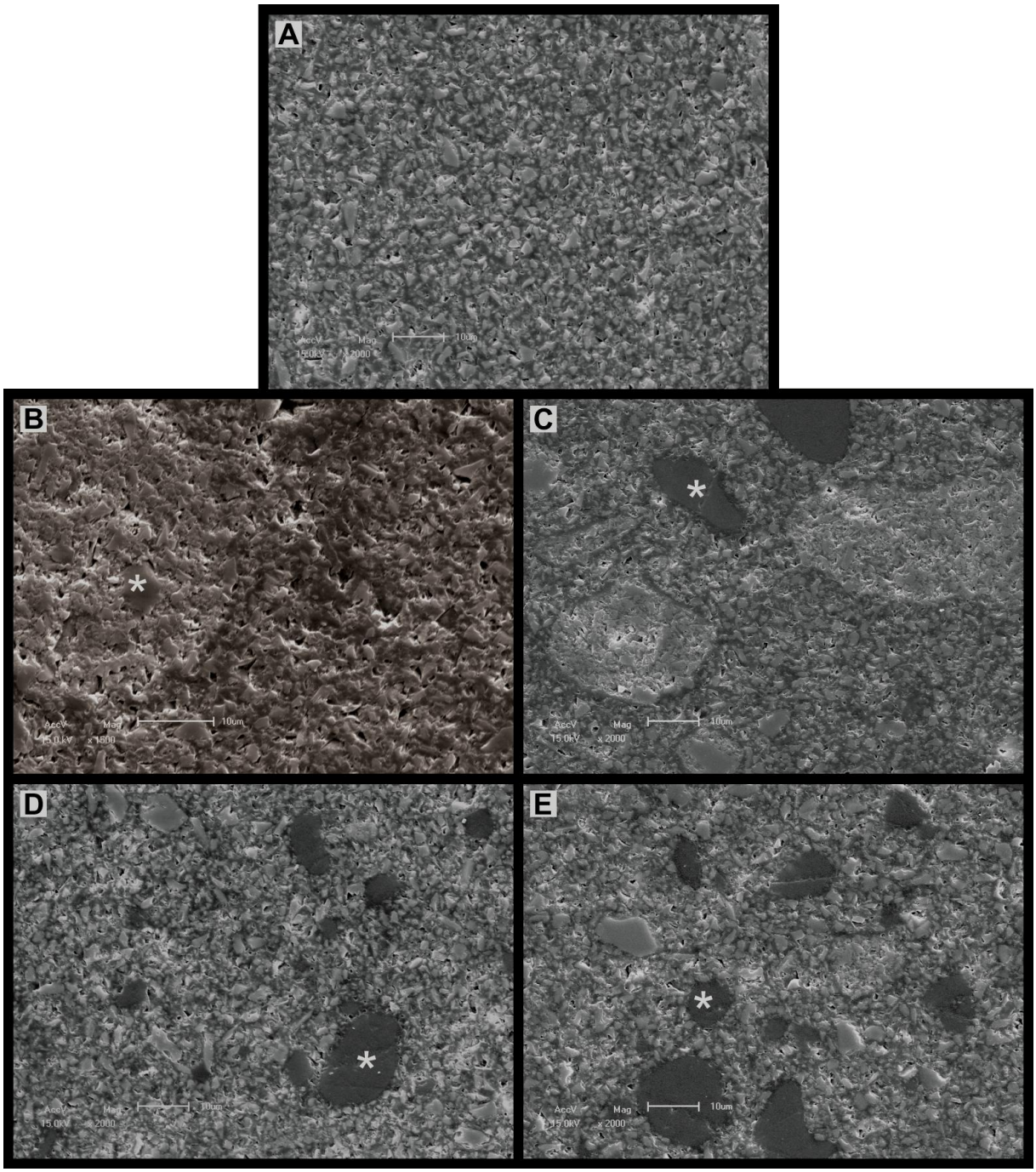

Figure 2

3 ARTIGO 2[*] - Properties of particulate resin luting agents with phosphate and carboxylic functional methacrylates as coupling agents

[*] Artigo redigido segundo o Guia para Autores do Journal of the Mechanical Behavior of Biomedical Materials, disponível em: http://www.elsevier.com/wps/find/journaldescription.cws_home/711005/authorinstructions
Acesso em: 03 de novembro de 2010.

Properties of particulate resin luting agents with phosphate and carboxylic functional methacrylates as coupling agents

Luciano V. Habekost[a], Guilherme B. Camacho[a], Giana S. Lima[a], Fabrício A. Ogliari[b], Evandro Piva[a], Rafael R. Moraes[a]

[a]School of Dentistry, Federal University of Pelotas;
R. Gonçalves Chaves 457, 96015-560, Pelotas-RS, Brazil

[b]Materials Engineering School, Federal University of Pelotas, RS, Brazil;
R. Félix da Cunha 809, 96010-000, Pelotas-RS, Brazil

Corresponding author:
Prof. Rafael R. Moraes
School of Dentistry, Federal University of Pelotas
R. Gonçalves Chaves 457, 96015-560, Pelotas-RS, Brazil
Telephone/Fax: 55 53 3222.6690 (moraesrr@gmail.com)

Properties of particulate resin luting agents with phosphate and carboxylic functional methacrylates as coupling agents

Short title: *Filler treatment vs. resin luting agents properties*

Keywords: acidic methacrylates; coupling agents; inorganic filler; resin cements; silane; surface treatment.

Abstract

The aim of this study was to investigate properties of dental resin luting agents using silane [3-(trimethoxysilyl)propyl methacrylate – TSPM], phosphoric acid methacrylate [mono/bis(methacryloyloxyethyl (di)hydrogen phosphate) – PAM] or carboxylic acid methacrylate [mono-2-(methacryloyloxy)ethyl maleate – CAM] as coupling agents between the inorganic and organic phases. Ba-B-Al-Si microparticles (3 μm) and SiO_2 nanoparticles (7 nm) were coated with 5% mass fraction of TSPM, PAM or CAM (Control = no filler treatment). A photo-curable Bis-GMA/TEGDMA co-monomer was loaded with 60% mass fraction of inorganic fillers (59:1 mass ratio of micro- and nanoparticles). Degree of conversion (DC) was evaluated by mid-infrared spectroscopy. Flexural strength (σ) and modulus (E_f) were measured on three-point bending mode. The Knoop hardness number (KHN) was assessed through a microindenter. Film thickness (FT) was measured by loading the resin luting agents between glass plates. Dispersion/interaction of the filler particles with the resin phase was assessed by scanning electron microscopy (SEM). No significant differences in DC were observed. For σ and E_f, TSPM > CAM > control > PAM. For KHN, TSPM > CAM > PAM = control. For FT, TSPM < control < CAM < PAM. The SEM analysis revealed clustering of nanoparticles for all groups and better interaction between the organic–inorganic phases for TSPM and CAM. The use of TSPM generated agents with improved properties as compared with the acidic methacrylates, with CAM showing better performance than PAM. The use of PAM generated agents with properties usually poorer compared with the material with no coupling agent.

Introduction

Dental resin luting agents consist of a resin matrix mixed with reinforcing inorganic particles; a coupling agent mediates the bonding between these two phases. The filler–polymer interaction is expected to affect the material mainly by influencing the dispersion of the particles within the resin matrix (Thio et al., 2004), affecting properties as monomer conversion, viscosity and film thickness. The interfacial strength is also expected to affect mechanical processes during macroscopic deformation, leading to better load transfer, toughening and increased wear resistance (Lim et al., 2002; Mohsen and Craig, 1995).

The most common coupling agents in dental composites are organo-silanes (Tham et al., 2010). These agents contain a trialkoxysilane function on one end for bonding to the silica-containing fillers, and a methacrylate group on the other end to make the fillers compatible with the resin. The alkoxy groups of silanes are hydrolyzed into silanol groups to bond with silica through the formation of siloxane bonds (Debnath et al., 2003; Matinlinna et al., 2004), as shown in Figure 1. It has been suggested, however, that the breakdown of the filler–polymer interface may be one of the main causes of failures of dental composites (Drummond, 2008), as hydrolysis of the siloxane bonds may lead to filler dislodgment (Soderholm and Shang, 1993). Another limitation of silanes is the dependence on the presence of silica in the inorganic fillers. Silica is radiolucent and has been partially substituted by heavy metal-containing glasses or minerals in dental composites (Amirouche-Korichi et al., 2009).

Other potential coupling agents for resin composites are acidic methacrylates. Functional acidic monomers are characterized by three segments: a polymerizable group, a spacer, and an acid termination (Ogliari et al., 2008). It has been shown that functional groups capable of releasing one or more protons, such as carboxyl and phosphate groups, may bond to metal oxides (Almilhatti et al., 2009; Behr et al., 2003; Masuno et al., 2010; Nothdurft et al., 2009; Van Landuyt et al., 2008). Likewise, the use of functional monomers as coupling agents could potentially allow bonding to inorganic fillers not containing silica, although this effect is still unknown.

The aim of this study was to investigate the potential use of acidic monomers as coupling agents for particulate dental resin cements. The null-hypothesis to the tested were: (I) the properties of the resin luting agents cements would be independent of the filler treatment, and (II) there would be no differences in the filler–resin interaction for agents obtained using the different coupling agents.

Material and Methods

Filler treatments

Ba-B-Al-Si glass microparticles (Schott, Mainz, Germany – d_{50} = 3±1 μm) and silica nanoparticles (Aerosil 380; Degussa, Germany – 7 nm average size) were used. The particles were submitted to one of the following surface treatments, as shown in Table 1: none (control), coating with an organo-silane coupling agent, a carboxylic acid methacrylate monomer, or a phosphoric acid methacrylate monomer (Lima et al., 2008). The molecular structure of the coupling agents is shown in Figure 2. The amount of coating material was set at 5% mass fraction related to the mass of the inorganic fillers. The coupling agents were diluted in ethanol, the particles soaked into the solution and left to dry at 54°C for 24 h to assure complete solvent removal. After storage, the fillers were sieved through a 150-μm sieve.

Formulation of the resin cements

A model dimethacrylate co-monomer blend based on a 1:1 mass ratio of 2,2-bis[4-(2-hydroxy-3-methacryloxypropoxy)phenyl]propane (Bis-GMA) and triethyleneglycol dimethacrylate (TEGDMA) (Esstech Inc., Essington, PA, USA) was loaded with a 0.4% mass fraction of camphorquinone (Esstech Inc.), 0.8% mass fraction of ethyl 4-dimethylamino benzoate (Sigma-Aldrich, St. Louis, MO, USA), and 0.1% mass fraction of butylated hydroxytoluene (Sigma-Aldrich) as radical scavenger. All chemicals were used as received. Four resin luting agents were obtained by loading the model co-monomer with a 60% mass fraction of the fillers submitted to one of the treatments described before. The filler system was added at a 59:1 mass ratio of micro- and nanoparticles. The particles were incorporated by

intensive manual mixing followed by mechanical stirring with a motorized mixer. In order to assure the adequate dispersion of the filler system, the materials were sonicated for 1 h.

Degree of conversion

The degree of conversion (DC) was measured using Fourier transform infrared (FTIR) spectroscopy (Prestige21; Shimadzu, Tokyo, Japan), equipped with an attenuated total reflectance (ATR) device. The unpolymerized materials were placed direct on the ATR cell and the unpolymerized spectra was obtained. The readings were taken under the following conditions: 32 scan co-addition, 4 cm^{-1} resolution, and 2.8 mm/s mirror speed. Photoactivation was then carried out for 40 s using a LED unit (Radii; SDI, Bayswater, Victoria, Australia) with 600 mW/cm^2 irradiance. The light guide tip was positioned 2 mm away from the material. The diameter of the specimens was restricted to match the diameter of the light guide. The DC (%) was evaluated in the absorbance mode using a baseline technique (Rueggeberg et al., 1990), considering the intensity of C=C stretching vibration (peak height) at 1635 cm^{-1} and, as an internal standard, using the symmetric ring stretching at 1608 cm^{-1}. Five specimens were tested for each cement.

Flexural strength and modulus

Flexural tests were performed using twenty bar specimens with dimensions of 12 × 2 × 2 mm (8 mm span width). The resin luting agent was placed into the stainless steel/glass mold, covered with a Mylar strip and photocured using two irradiations of 40 s on each side. The specimens were dry stored in lightproof containers at 37°C. 24 h after irradiation, a three-point bending test was carried out on a mechanical testing machine (DL500; EMIC, São José dos Pinhais, PR, Brazil) at a crosshead speed of 0.5 mm/min. Flexural strength (σ) and flexural modulus (E_f) were calculated from the load-displacement trace.

Hardness

The materials were placed into cylinder-shaped metal molds (5 mm inner diameter × 2 mm thick), covered with a Mylar strip and light-activated for 40 s on each surface. The specimens were dry stored in lightproof containers at 37^{o}C, for 24 h, then wet-ground with 800-, 1000-, 1200- and 1500-grit SiC abrasive papers. Three readings were performed on each specimen through a microindenter (FM-700; Future-Tech, Kawasaki, Japan), under a load of 25 g and a dwell time of 5 s. The Knoop hardness number (KHN, kgf/mm^2) for each specimen was recorded as the average of the three indentations. Five specimens were tested for each luting agent.

Film thickness

Two optically flat square glass plates, each 5 mm thick, and having a contact surface area of 200 mm^2 were used. The combined thickness of the glass plates stacked in contact was measured (reading A) with a digital caliper (MDC-Lite; Mitutoyo, Suzano, SP, Brazil), accurate to 0.001 mm. Then, 0.1 mL of resin cement was placed centrally between the plates, and a constant load of 150 N was carefully applied vertically and centrally via the top plate, for 180 s. After this period, light irradiation was performed for 40 s in order to stabilize the specimen. The combined thickness of the two glass plates and the luting agent film was measured (reading B). Film thickness was recorded as the difference between reading B and reading A. Five specimens were tested for each luting agent.

SEM analysis

In order to observe the dispersion and interaction of the filler particles within the resin phase, cylinder-shaped specimens (5 mm diameter × 1 mm thick) were embedded in epoxy resin and wet-polished with 600-, 1200-, 1500-, 2000- and 2500-grit SiC papers and with 3, 1, 0.25 and 0.1 μm diamond polishing suspensions. The specimens were coated with gold and the polished surfaces examined by scanning electron microscopy – SEM (SSX-550; Shimadzu) at 15 kV.

Statistical analysis

Data from each test were submitted to one-way ANOVA followed by the Tukey's *post-hoc* test ($P < 0.05$).

Results

Results for all evaluations are presented in Table 2. No significant differences among the filler treatments were detected in the DC analysis ($P = 0.127$). For flexural strength, all groups presented significantly different results as compared to each other: TSPM > CAM > control > PAM ($P < 0.001$). Likewise, for flexural modulus, TSPM was significantly higher than CAM ($P< 0.001$), which was significantly higher than the control group ($P = 0.023$); the group PAM showed again significantly lower values than all the other groups ($P < 0.001$). The group TSPM also showed significantly higher KHN than all the other groups ($P < 0.001$); CAM showed intermediate results for KHN, while the groups PAM and control showed the lowest KHN values. For film thickness, all filler treatments showed results significantly different compared to each other: TSPM < control < CAM < PAM ($P \leq 0.03$).

SEM pictures of the polished cement surfaces are shown in Figure 3. Irrespective of the surface treatment of the fillers, clusters formed by the nanoparticles were evident. In addition, voids between the fillers and the organic resin matrix were observed, owing to the detachment of fillers during the polishing procedures. The areas caused by dislodgement and loss of fillers were more evident for the control and PAM groups. The presence of these areas was less frequent for the TSPM group as compared with the other surface treatments.

Discussion

The first null-hypothesis tested was rejected, as resin cements with functional methacrylates as coupling agents presented a wide range of properties, usually poorer as compared with the silane-containing cement. The presence of residual acidic methacrylates is usually associated with negative effects on the DC due to the

ability of functional monomers in quenching free radicals (Sanares et al., 2001; Suh et al., 2003). Radicals terminated by an acid group are also less reactive than free radicals derived from unmodified monomers, reducing the polymerization rate (Adusei et al., 2003). However, treating the particles with acidic monomers had no significant effect on the DC. This finding is most likely related to the low amount of coupling agent used in the study. A previous investigation showed that substantial reductions in DC occurred mainly in the presence of high concentration of acidic monomers, and that the effect was more stressed in self-cured materials (which show slower cure) due the deactivation of the amine co-initiator (Suh et al., 2003).

Materials treated with TSPM clearly showed better mechanical properties compared with either acidic methacrylates. This is the first time this result is described, as no previous investigation on the use of acidic methacrylates as coating agents could be found. Previous studies have reported the beneficial effects of coating the filler particles with silanes (Ikejima et al., 2003; Mohsen and Craig, 1995). This finding might be related to the fact that the bond of TSPM with the fillers relies on the formation of strong covalent siloxane bonds (Figure 1), whereas the interaction of the acidic methacrylates with fillers probably relies on a weaker ionic interaction between the acid and silanol groups (mechanism proposed in Figure 4). Comparing the results of the two functional monomers, the performance of CAM was better compared with PAM. The behavior of PAM, as a matter of fact, was sometimes poorer compared with the control group, with no coupling agent. One possible explanation for this result is PAM has a non-reacted acid hydroxyl, which may render the monomer too acid even after coating, therefore interfering with the properties of the cement.

In the SEM analysis, voids due to filler detachment were more frequent for the groups control and PAM, suggesting poor interaction between the inorganic and organic phases. Thus the second null-hypothesis is also rejected. This poorer interaction may be another cause of the deleterious effects on flexural strength and modulus, as well on hardness, observed for the group PAM. The areas with poor bond between the phases may have served as spots for stress concentration during the mechanical testing. Although the results observed for the group CAM were better as compared with PAM, the group TSPM showed the best results for all mechanical conditions. This result, in addition to the SEM analysis, indicate a more

homogeneous dispersion and better filler–resin interaction when TSPM was used as coupling agent.

During the mixing of the luting agents, variations in the interfacial chemistry caused noticeable differences in how readily the fillers could be incorporated into the resin, as well in the final consistency of the pastes. Potential increases in filler loading in composite pastes have indeed been associated with variations in the silica surface chemistry and subsequent changes in particle–particle and particle–resin interactions (Wilson et al., 2005). A significant reduction in the surface pH has been described when a silica-based ceramic was treated with acid, indicating an increase in the concentration of H^+ ions in the surface (Foxton et al., 2003). When the acidic methacrylates were used, it is possible the same effect occurred, hindering the incorporation of the fillers. As the acidity of the acidic monomers is defined by their dissociation constants (pKa= 10^{-5} for CAM and 10^{-3} for PAM) (Suh et al., 2003), the lower pH of PAM may have enhanced this effect, causing a polarity incompatibility. A previous study have indeed described that CAM and PAM derivatives may shown distinct bonding performances to metal oxides (Masuno et al., 2010).

The film thickness was also influenced by the coating material used. The lower film thickness for TSPM may be a result of the better wettability of the TSPM-coated particles within the resin phase. The use of silanes has been associated with a reduction in the amount of co-monomer needed to incorporate a given amount of inorganic filler and obtain a given consistency (Lim et al., 2002; Mohsen and Craig, 1995). However, the results for film thickness did not follow the same trend for mechanical data; the film thickness for the group CAM was higher than for the control luting agent. This finding suggests filler–resin interactions other than the wettability of the particles solely contribute to the resulting film thickness of the material.

The data from the different tests and SEM images suggest that resin–particle interaction and their interface have a significant impact on properties of particulate resin luting agents. Under stress loading, the connectivity of the filler with the polymer matrix is even more important than the ultimate strength of the polymer, as a good link may halt the crack propagation in the matrix surrounding the filler (Lin et al., 2000). Interestingly, irrespective of the surface coating, clustering of nanoparticles was always present. Although for some examples the mechanical

properties of particle agglomerates can be relatively low (Lim et al., 2002), the inter-particle spaces are very small inside the clusters. Therefore, provided that strong connective forces between the nanoparticles themselves and between the nanoparticles with the resin are obtained, these areas may have a protective effect in the structure. Poor connective forces, on the other hand, may lead the clusters to act as spots for stress concentration within the cement, impairing the mechanical properties.

Although the best results were observed for TSPM, the hydrolysis of the Si–O–Si bonds and of the ester linkage that serves as the silane-resin bond is a well-known phenomenon which is expected to weaken the polymer-filler interface during aging (Drummond, 2008). Therefore, other filler treatments should still be evaluated. Different concentration of acidic monomers, acidic functionalities and perhaps the combined use of organo-silanes and acidic methacrylates could be investigated.

Conclusion

The use of acidic methacrylates to couple the organic and inorganic phases of particulate resin luting agents generates materials with poorer properties as compared with cements having an organo-silane as coupling agent.

References

1. Adusei, G., Deb, S., Nicholson, J.W., Mou, L.Y., Singh, G., 2003. Polymerization behavior of an organophosphorus monomer for use in dental restorative materials. J Appl Polym Sci 88, 565-569.

2. Almilhatti, H.J., Giampaolo, E.T., Vergani, C.E., Machado, A.L., Pavarina, A.C., Betiol, E.A., 2009. Adhesive bonding of resin composite to various Ni-Cr alloy surfaces using different metal conditioners and a surface modification system. J Prosthodont 18, 663-669.

3. Amirouche-Korichi, A., Mouzali, M., Watts, D.C., 2009. Effects of monomer ratios and highly radiopaque fillers on degree of conversion and shrinkage-strain of dental resin composites. Dent Mater 25, 1411-1418.

4. Behr, M., Rosentritt, M., Groger, G., Handel, G., 2003. Adhesive bond of veneering composites on various metal surfaces using silicoating, titanium-coating or functional monomers. J Dent 31, 33-42.

5. Debnath, S., Wunder, S.L., McCool, J.I., Baran, G.R., 2003. Silane treatment effects on glass/resin interfacial shear strengths. Dent Mater 19, 441-448.

6. Drummond, J.L., 2008. Degradation, fatigue, and failure of resin dental composite materials. J Dent Res 87, 710-719.

7. Foxton, R.M., Nakajima, M., Hiraishi, N., Kitasako, Y., Tagami, J., Nomura, S., Miura, H., 2003. Relationship between ceramic primer and ceramic surface pH on the bonding of dual-cure resin cement to ceramic. Dent Mater 19, 779-789.

8. Ikejima, I., Nomoto, R., McCabe, J.F., 2003. Shear punch strength and flexural strength of model composites with varying filler volume fraction, particle size and silanation. Dent Mater 19, 206-211.

9. Lim, B.S., Ferracane, J.L., Condon, J.R., Adey, J.D., 2002. Effect of filler fraction and filler surface treatment on wear of microfilled composites. Dent Mater 18, 1-11.

10. Lima, G.S., Ogliari, F.A., da Silva, E.O., Ely, C., Demarco, F.F., Carreno, N.L., Petzhold, C.L., Piva, E., 2008. Influence of water concentration in an experimental self-etching primer on the bond strength to dentin. J Adhes Dent 10, 167-172.

11. Lin, C.T., Lee, S.Y., Keh, E.S., Dong, D.R., Huang, H.M., Shih, Y.H., 2000. Influence of silanization and filler fraction on aged dental composites. J Oral Rehabil 27, 919-926.

12. Masuno, T., Koizumi, H., Ishikawa, Y., Nakayama, D., Yoneyama, T., Matsumura, H., 2010. Effect of acidic monomers on bonding to SUS XM27 stainless steel, iron, and chromium with a tri-n-butylborane-initiated acrylic resin. J Adhes Dent, *in press*. doi: 10.3290/j.jad.a18392.

13. Matinlinna, J.P., Lassila, L.V., Ozcan, M., Yli-Urpo, A., Vallittu, P.K., 2004. An introduction to silanes and their clinical applications in dentistry. Int J Prosthodont 17, 155-164.

14. Mohsen, N.M., Craig, R.G., 1995. Effect of silanation of fillers on their dispersability by monomer systems. J Oral Rehabil 22, 183-189.

15. Nothdurft, F.P., Motter, P.J., Pospiech, P.R., 2009. Effect of surface treatment on the initial bond strength of different luting cements to zirconium oxide ceramic. Clin Oral Investig 13, 229-235.

16. Ogliari, F.A., da Silva, E.O., Lima G da, S., Madruga, F.C., Henn, S., Bueno, M., Ceschi, M.A., Petzhold, C.L., Piva, E., 2008. Synthesis of phosphate monomers and bonding to dentin: esterification methods and use of phosphorus pentoxide. J Dent 36, 171-177.

17. Rueggeberg, F.A., Hashinger, D.T., Fairhurst, C.W., 1990. Calibration of FTIR conversion analysis of contemporary dental resin composites. Dent Mater 6, 241-249.

18. Sanares, A.M., Itthagarun, A., King, N.M., Tay, F.R., Pashley, D.H., 2001. Adverse surface interactions between one-bottle light-cured adhesives and chemical-cured composites. Dent Mater 17, 542-556.

19. Soderholm, K.J., Shang, S.W., 1993. Molecular orientation of silane at the surface of colloidal silica. J Dent Res 72, 1050-1054.

20. Suh, B.I., Feng, L., Pashley, D.H., Tay, F.R., 2003. Factors contributing to the incompatibility between simplified-step adhesives and chemically-cured or dual-cured composites. Part III. Effect of acidic resin monomers. J Adhes Dent 5, 267-282.

21. Tham, W.L., Chow, W.S., Ishak, Z.A.M., 2010. The Effect of 3-(Trimethoxysilyl) Propyl Methacrylate on the Mechanical, Thermal, and Morphological Properties of Poly(methyl methacrylate)/Hydroxyapatite Composites. Journal of Applied Polymer Science 118, 218-228.

22. Thio, Y.S., Argon, A.S., Cohen, R.E., 2004. Role of interfacial adhesion strength on toughening polypropylene with rigid particles. Polymer 45, 3139-3147.

23. Van Landuyt, K.L., Yoshida, Y., Hirata, I., Snauwaert, J., De Munck, J., Okazaki, M., Suzuki, K., Lambrechts, P., Van Meerbeek, B., 2008. Influence of the chemical structure of functional monomers on their adhesive performance. J Dent Res 87, 757-761.

24. Wilson, K.S., Zhang, K., Antonucci, J.M., 2005. Systematic variation of interfacial phase reactivity in dental nanocomposites. Biomaterials 26, 5095-5103.

Tables

Table 1. Filler treatments tested in the study

Filler treatment	Coupling agent*	Manufacturer	Group code
None	-	-	Control
Silane	3-(trimethoxysilyl)propyl methacrylate	Sigma-Aldrich	TSPM
Carboxylic acid methacrylate	mono-2-(methacryloyloxy)ethyl maleate	Sigma-Aldrich	CAM
Phosphoric acid methacrylate	equimolar mixture of methacryloyloxyethyl dihydrogen phosphate / bis(methacryloyloxyethyl) hydrogen phosphate	Synthesized as described elsewhere (Lima et al., 2008)	PAM

*The proposed mechanisms for the bond between the coupling agents and the inorganic glass fillers are shown in Figures 1 and 4.

Table 2. Means (SD) for degree of conversion (DC), flexural strength (σ), elastic modulus (E_f), hardness (KHN) and film thickness (FT)

	Filler treatment			
	Control	TSPM	CAM	PAM
DC, %	59.0 (0.7) ^{A}	54.1 (0.5) ^{A}	58.1 (6.2) ^{A}	59.7 (4.0) ^{A}
σ, MPa	40.0 (4) ^{C}	107.0 (16) ^{A}	56.0 (12) ^{B}	23.0 (4) ^{D}
E_f, GPa	1.55 (0.2) ^{C}	2.04 (0.2) ^{A}	1.72 (0.2) ^{B}	0.8 (0.1) ^{D}
KHN, kgf/mm^2	16.8 (1.7) ^{C}	34.5 (2.2) ^{A}	23.6 (1.2) ^{B}	18.2 (1.4) ^{C}
FT, µm	10.2 (1.8) ^{C}	4.2 (2.6) ^{D}	17.2 (3.4) ^{B}	38.6 (4.0) ^{A}

Distinct letters in a same row indicate significant differences for filler treatment ($P < 0.05$).

Figure Legends

Figure 1. The reaction of TSPM with the glass filler involves four steps. Initially, hydrolysis of the methoxy label groups occurs. Condensation to oligomers follows. The oligomers then hydrogen bond with the hydroxyl groups from the filler. Finally, as the silane dries, a covalent bond with the substrate is formed with concomitant loss of water.

Figure 2. Molecular structure of the coupling agents used in the study: (A) 3-(trimethoxysilyl)propyl methacrylate; (B) mono-2-(methacryloyloxy)ethyl maleate; (C) methacryloyloxyethyl dihydrogen phosphate / bis(methacryloyloxyethyl) hydrogen phosphate.

Figure 3. SEM pictures of the polished cements surfaces: TSPM (A), CAM (B), PAM (C) and control (D). Asterisks indicate nanoparticle clustering; arrows indicate cracks and voids between the fillers and resin phase.

Figure 4. Proposed mechanism for the bond between the carboxylic (A) and phosphoric (B) acid methacrylate monomers and the glass fillers based on an ionic interaction between the acid and silanol groups. Note the non-reacted phosphoric acid hydroxyl in B.

Figures

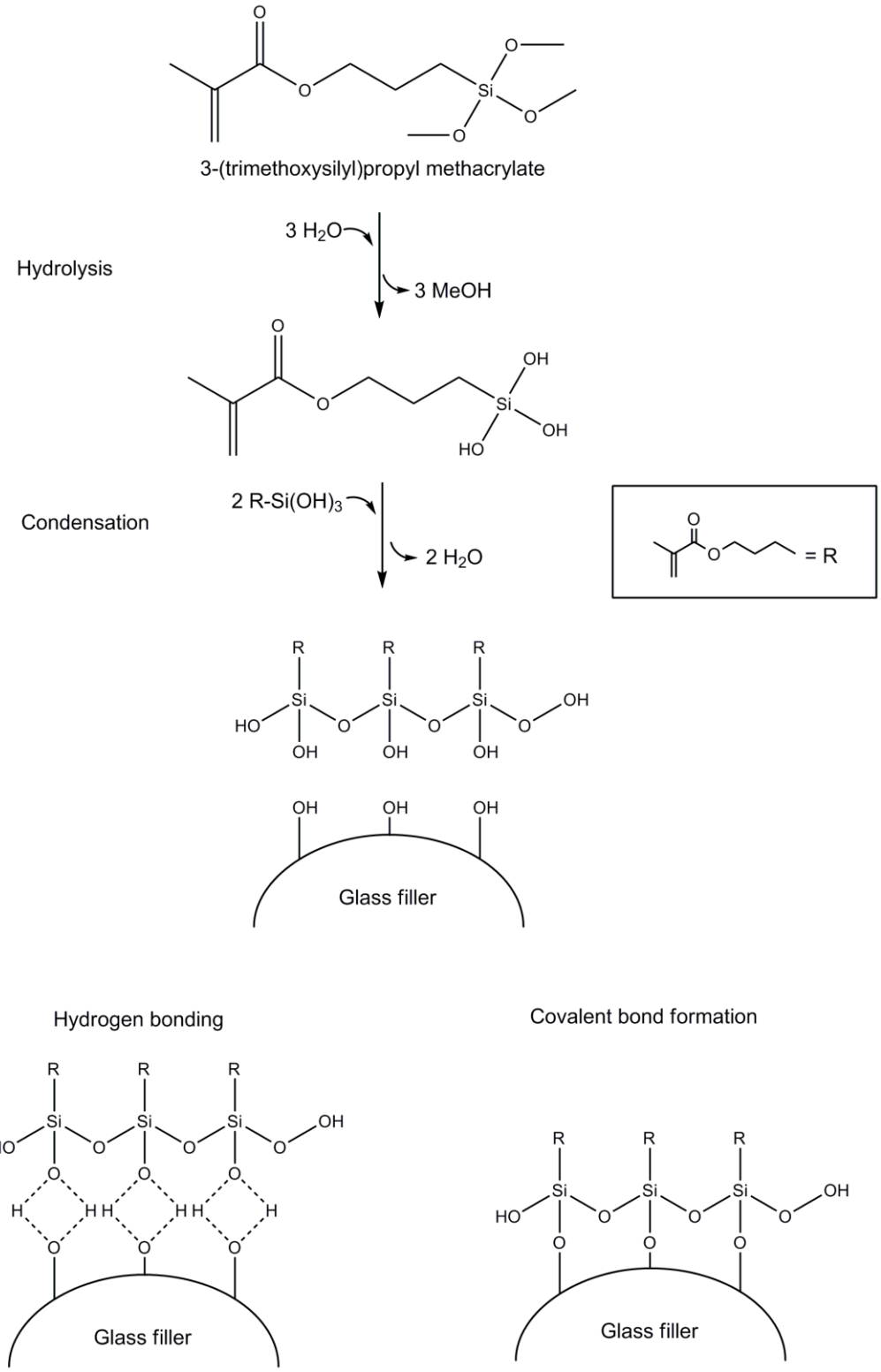

Figure 1

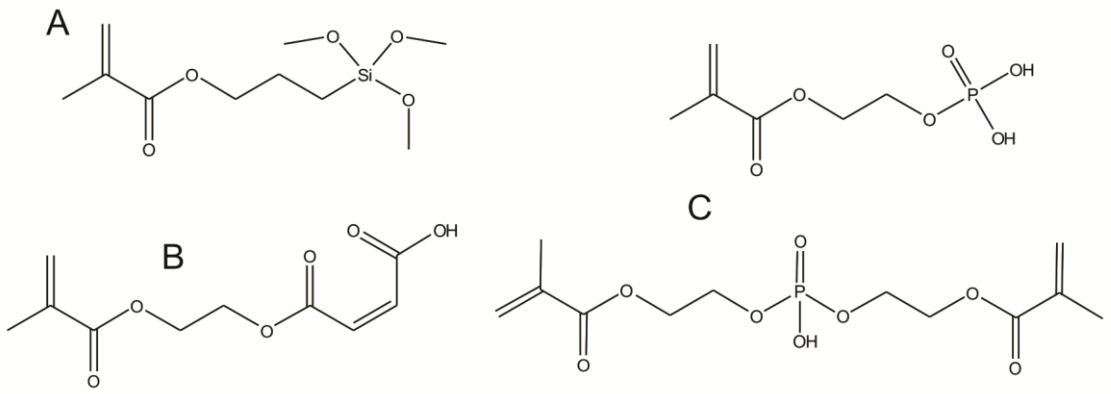

Figure 2

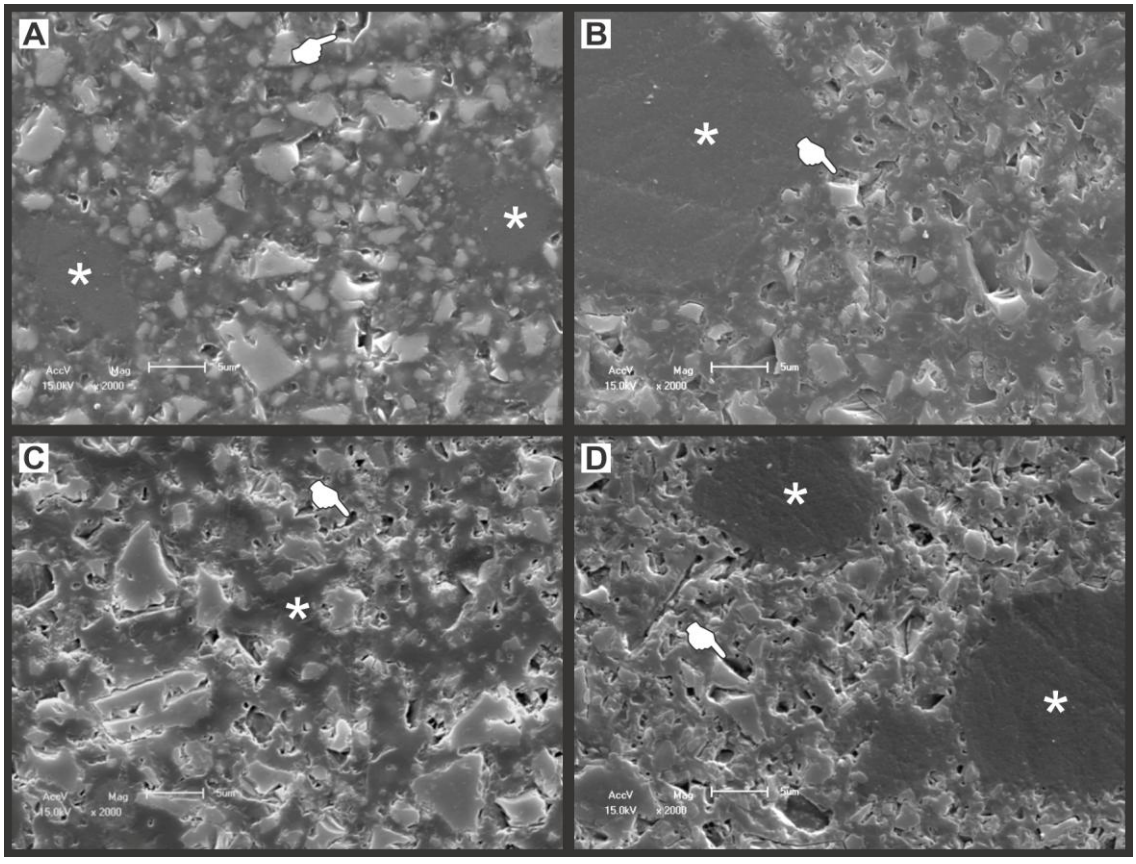

Figure 3

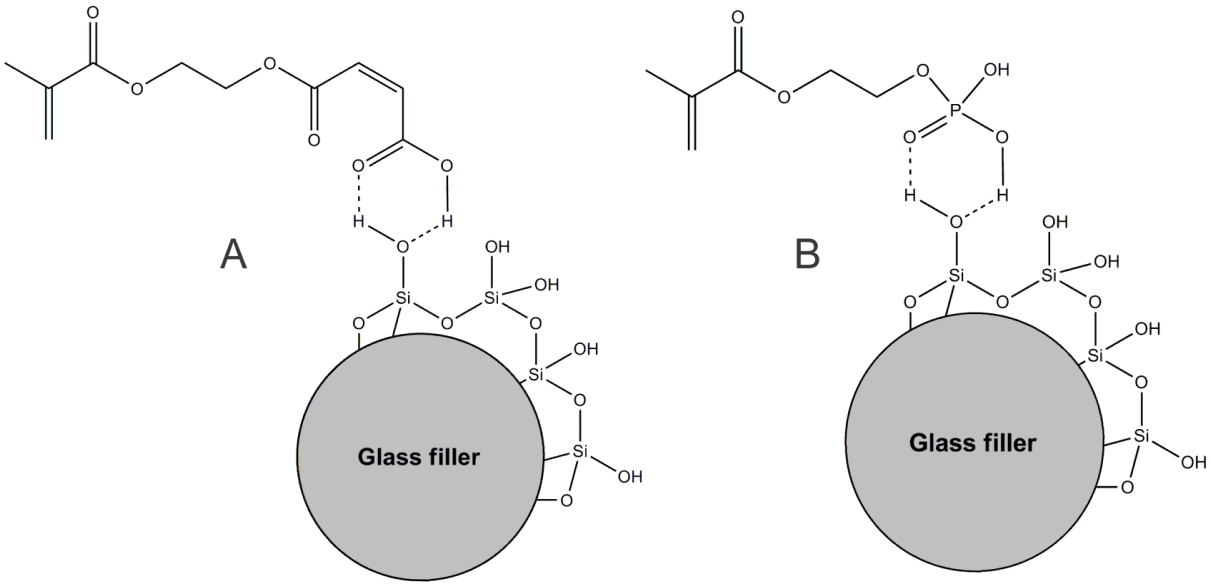

Figure 4

4 CONCLUSÕES

A incorporação criteriosa de nanopartículas de sílica silanizada pode melhorar as propriedades dos cimentos resinosos híbridos. Entretanto, acréscimos de nanopartículas acima de 2,5% (em massa) devem ser evitados; pois, em maiores porcentagens, apresentam caráter prejudicial às propriedades dos cimentos.

A utilização de silano como agente de união entre as fases orgânica e inorgânica de cimentos resinosos híbridos originou materiais com propriedades superiores aos materiais que utilizaram monômeros ácidos para o mesmo fim.

A incorporação de nanopartículas à carga de cimentos resinosos está associada à formação de aglomerados das mesmas.

5 REFERÊNCIAS

Addison, O., P. M. Marquis*, et al.* Resin elasticity and the strengthening of all-ceramic restorations. **Journal of Dental Research**, v.86, n.6, Jun, p.519-23. 2007.

Adusei, G., S. Deb*, et al.* Polymerization behavior of an organophosphorus monomer for use in dental restorative materials. **Journal of Applied Polymer Science**, v.88, n.2, p.565-9. 2003.

Almilhatti, H. J., E. T. Giampaolo*, et al.* Adhesive bonding of resin composite to various Ni-Cr alloy surfaces using different metal conditioners and a surface modification system. **Journal of Prosthodontics**, v.18, n.8, Dec, p.663-9. 2009.

Amirouche-Korichi, A., M. Mouzali*, et al.* Effects of monomer ratios and highly radiopaque fillers on degree of conversion and shrinkage-strain of dental resin composites. **Dental Materials**, v.25, n.11, Nov, p.1411-8. 2009.

Behr, M., M. Rosentritt*, et al.* Adhesive bond of veneering composites on various metal surfaces using silicoating, titanium-coating or functional monomers. **Journal of Dentistry**, v.31, n.1, Jan, p.33-42. 2003.

Braga, R. R., P. F. Cesar*, et al.* Mechanical properties of resin cements with different activation modes. **Journal of Oral Rehabilitation**, v.29, n.3, Mar, p.257-62. 2002.

Chan, D. C., H. W. Titus*, et al.* Radiopacity of tantalum oxide nanoparticle filled resins. **Dental Materials**, v.15, n.3, May, p.219-22. 1999.

Chen, M. H. Update on dental nanocomposites. **Journal of Dental Research**, v.89, n.6, Jun, p.549-60. 2010.

Chung, K. H. e E. H. Greener. Correlation between degree of conversion, filler concentration and mechanical properties of posterior composite resins. **Journal of Oral Rehabilitation**, v.17, n.5, Sep, p.487-94. 1990.

Curtis, A. R., W. M. Palin*, et al.* The mechanical properties of nanofilled resin-based composites: the impact of dry and wet cyclic pre-loading on bi-axial flexure strength. **Dental Materials**, v.25, n.2, Feb, p.188-97. 2009.

Debnath, S., S. L. Wunder*, et al.* Silane treatment effects on glass/resin interfacial shear strengths. **Dental Materials**, v.19, n.5, Jul, p.441-8. 2003.

Drummond, J. L. Degradation, fatigue, and failure of resin dental composite materials. **Journal of Dental Research**, v.87, n.8, Aug, p.710-9. 2008.

Faria, A. C., U. M. Benassi*, et al.* Analysis of the relationship between the surface hardness and wear resistance of indirect composites used as veneer materials. **Brazilian Dental Journal**, v.18, n.1, p.60-4. 2007.

Fleming, G. J. e O. Narayan. The effect of cement type and mixing on the bi-axial fracture strength of cemented aluminous core porcelain discs. **Dental Materials**, v.19, n.1, Jan, p.69-76. 2003.

Foxton, R. M., M. Nakajima*, et al.* Relationship between ceramic primer and ceramic surface pH on the bonding of dual-cure resin cement to ceramic. **Dental Materials**, v.19, n.8, Dec, p.779-89. 2003.

Habekost, L. V., G. B. Camacho*, et al.* Fracture resistance of thermal cycled and endodontically treated premolars with adhesive restorations. **Journal of Prosthetic Dentistry**, v.98, n.3, Sep, p.186-92. 2007.

_____. Tensile bond strength and flexural modulus of resin cements--influence on the fracture resistance of teeth restored with ceramic inlays. **Operative Dentistry**, v.32, n.5, Sep-Oct, p.488-95. 2007.

Hosseinalipour, M., J. Javadpour*, et al.* Investigation of mechanical properties of experimental Bis-GMA/TEGDMA dental composite resins containing various mass fractions of silica nanoparticles. **Journal of Prosthodontics**, v.19, n.2, Feb, p.112-7. 2010.

Ikejima, I., R. Nomoto*, et al.* Shear punch strength and flexural strength of model composites with varying filler volume fraction, particle size and silanation. **Dental Materials**, v.19, n.3, May, p.206-11. 2003.

International Standard ISO 4049: Dentistry — Polymer-based restorative materials, p.5. 2009.

Jorgensen, K. D., P. Horsted*, et al.* Abrasion of class 1 restorative resins. **Scandinavian Journal of Dental Research**, v.87, n.2, Apr, p.140-5. 1979.

Kim, J. W., L. U. Kim*, et al.* Size control of silica nanoparticles and their surface treatment for fabrication of dental nanocomposites. **Biomacromolecules**, v.8, n.1, Jan, p.215-22. 2007.

Kim, K. H., J. L. Ong*, et al.* The effect of filler loading and morphology on the mechanical properties of contemporary composites. **Journal of Prosthetic Dentistry**, v.87, n.6, Jun, p.642-9. 2002.

Lee, J. H., C. M. Um*, et al.* Rheological properties of resin composites according to variations in monomer and filler composition. **Dental Materials**, v.22, n.6, Jun, p.515-26. 2006.

Lee, J. Y., Q. L. Zhang*, et al.* Nanoparticle alignment and repulsion during failure of glassy polymer nanocomposites. **Macromolecules**, v.39, n.21, Oct 17, p.7392-7396. 2006.

Lim, B. S., J. L. Ferracane*, et al.* Effect of filler fraction and filler surface treatment on wear of microfilled composites. **Dental Materials**, v.18, n.1, Jan, p.1-11. 2002.

Lima, G. S., F. A. Ogliari*, et al.* Influence of water concentration in an experimental self-etching primer on the bond strength to dentin. **The Journal of Adhesive Dentistry**, v.10, n.3, Jun, p.167-72. 2008.

Lin, C. T., S. Y. Lee*, et al.* Influence of silanization and filler fraction on aged dental composites. **Journal of Oral Rehabilitation**, v.27, n.11, Nov, p.919-26. 2000.

Masuno, T., H. Koizumi*, et al.* Effect of acidic monomers on bonding to SUS XM27 stainless steel, iron, and chromium with a tri-n-butylborane-initiated acrylic resin. **The Journal of Adhesive Dentistry**, Feb 12, p.in press, doi: 10.3290/j.jad.a18392. 2010.

Matinlinna, J. P., L. V. Lassila*, et al.* An introduction to silanes and their clinical applications in dentistry. **International Journal of Prosthodontics**, v.17, n.2, Mar-Apr, p.155-64. 2004.

Mitra, S. B., D. Wu*, et al.* An application of nanotechnology in advanced dental materials.Journal of the American Dental Association, v.134, n.10, Oct, p.1382-90. 2003.

Mohsen, N. M. e R. G. Craig. Effect of silanation of fillers on their dispersability by monomer systems. **Journal of Oral Rehabilitation**, v.22, n.3, Mar, p.183-9. 1995.

Moraes, R. R., S. Goncalves Lde*, et al.* Nanohybrid resin composites: nanofiller loaded materials or traditional microhybrid resins? **Operative Dentistry**, v.34, n.5, Sep-Oct, p.551-7. 2009.

Nothdurft, F. P., P. J. Motter*, et al.* Effect of surface treatment on the initial bond strength of different luting cements to zirconium oxide ceramic. **Clinical Oral Investigations**, v.13, n.2, Jun, p.229-35. 2009.

Ogliari, F. A., E. O. Da Silva*, et al.* Synthesis of phosphate monomers and bonding to dentin: esterification methods and use of phosphorus pentoxide. **Journal of Dentistry**, v.36, n.3, Mar, p.171-7. 2008.

Rueggeberg, F. A., D. T. Hashinger*, et al.* Calibration of FTIR conversion analysis of contemporary dental resin composites. **Dental Materials**, v.6, n.4, Oct, p.241-9. 1990.

Sanares, A. M., A. Itthagarun*, et al.* Adverse surface interactions between one-bottle light-cured adhesives and chemical-cured composites. **Dental Materials**, v.17, n.6, Nov, p.542-56. 2001.

Shah, D., P. Maiti*, et al.* Effect of nanoparticle mobility on toughness of polymer nanocomposites. **Advanced Materials**, v.17, n.5, Mar 8, p.525-528. 2005.

Shah, M. B., J. L. Ferracane*, et al.* R-curve behavior and micromechanisms of fracture in resin based dental restorative composites. **Journal of the Mechanical Behavior of Biomedical Materials**, v.2, n.5, Oct, p.502-11. 2009.

Smith, K. A., S. Tyagi*, et al.* Healing surface defects with nanoparticle-filled polymer coatings: Effect of particle geometry. **Macromolecules**, v.38, n.24, Nov 29, p.10138-10147. 2005.

Soderholm, K. J. e S. W. Shang. Molecular orientation of silane at the surface of colloidal silica. **Journal of Dental Research**, v.72, n.6, Jun, p.1050-4. 1993.

Suh, B. I., L. Feng*, et al.* Factors contributing to the incompatibility between simplified-step adhesives and chemically-cured or dual-cured composites. Part III. Effect of acidic resin monomers. **The Journal of Adhesive Dentistry**, v.5, n.4, Winter, p.267-82. 2003.

Tham, W. L., W. S. Chow*, et al.* The Effect of 3-(Trimethoxysilyl) Propyl Methacrylate on the Mechanical, Thermal, and Morphological Properties of Poly(methyl methacrylate)/Hydroxyapatite Composites. **Journal of Applied Polymer Science**, v.118, n.1, Oct 5, p.218-228. 2010.

Thio, Y. S., A. S. Argon*, et al.* Role of interfacial adhesion strength on toughening polypropylene with rigid particles. **Polymer**, v.45, n.10, May 11, p.3139-3147. 2004.

Tian, M., Y. Gao*, et al.* Fabrication and evaluation of Bis-GMA/TEGDMA dental resins/composites containing nano fibrillar silicate. **Dental Materials**, v.24, n.2, Feb, p.235-43. 2008.

Turssi, C. P., J. L. Ferracane*, et al.* Wear and fatigue behavior of nano-structured dental resin composites. **Journal of Biomedical Materials Research Part B Applied Biomaterials**, v.78, n.1, Jul, p.196-203. 2006.

Van Landuyt, K. L., Y. Yoshida*, et al.* Influence of the chemical structure of functional monomers on their adhesive performance. **Journal of Dental Research**, v.87, n.8, Aug, p.757-61. 2008.

Wilson, K. S. e J. M. Antonucci. Interphase structure-property relationships in thermoset dimethacrylate nanocomposites. **Dental Materials**, v.22, n.11, Nov, p.995-1001. 2006.

Wilson, K. S., K. Zhang*, et al.* Systematic variation of interfacial phase reactivity in dental nanocomposites. **Biomaterials**, v.26, n.25, Sep, p.5095-103. 2005.

Yesil, Z. D., S. Alapati*, et al.* Evaluation of the wear resistance of new nanocomposite resin restorative materials. **Journal of Prosthetic Dentistry**, v.99, n.6, Jun, p.435-43. 2008.

APÊNDICES

Apêndice A – Relatórios dos ensaios referentes ao Artigo 1.

Relatórios do ensaio de resistência à mini-flexão e módulo de elasticidade*

Grupo 0%

UFPEL ensaio de flexão 3 pontos

Relatório de Ensaio

Máquina: Emic DL2000 Célula: Trd 24 Extensômetro: - Data: 27/11/2007 Hora: 09:13:14 Trabalho nº 0879
Programa: Tesc versão 3.01 Método de Ensaio: Mini-Flexão 3 pontos
Ident. Amostra: >>>Grupo: Luciano_grupo 1

Corpo de Prova	Area (mm2)	Tensão Máxima (MPa)	módulo elasticidade (MPa)
CP 1	0.55	166.71	2108.12
CP 2	0.61	162.90	2110.71
CP 3	0.58	163.21	2294.34
CP 4	0.61	168.65	2174.19
CP 5	0.66	135.84	1949.88
CP 6	0.57	157.43	2230.96
CP 7	0.62	133.42	2172.76
CP 8	0.60	161.55	2202.82
CP 9	0.59	146.11	2495.77
CP 10	0.60	153.57	2010.43
CP 11	0.71	125.84	1301.95
CP 12	0.76	136.62	1846.35
CP 13	0.55	157.18	1839.42
CP 14	0.61	111.32	1826.97
CP 15	0.66	116.58	1217.22
CP 16	0.67	134.47	1652.11
CP 17	0.74	127.36	1280.18
CP 18	0.72	135.17	1431.98
Número CPs	18	18	18
Média	0.6338	144.1	1897
Mediana	0.6083	141.4	1980
Desv.Padrão	0.06526	17.88	380.7
Coef.Var.(%)	10.30	12.41	20.07
Mínimo	0.5473	111.3	1217
Máximo	0.7589	168.6	2496

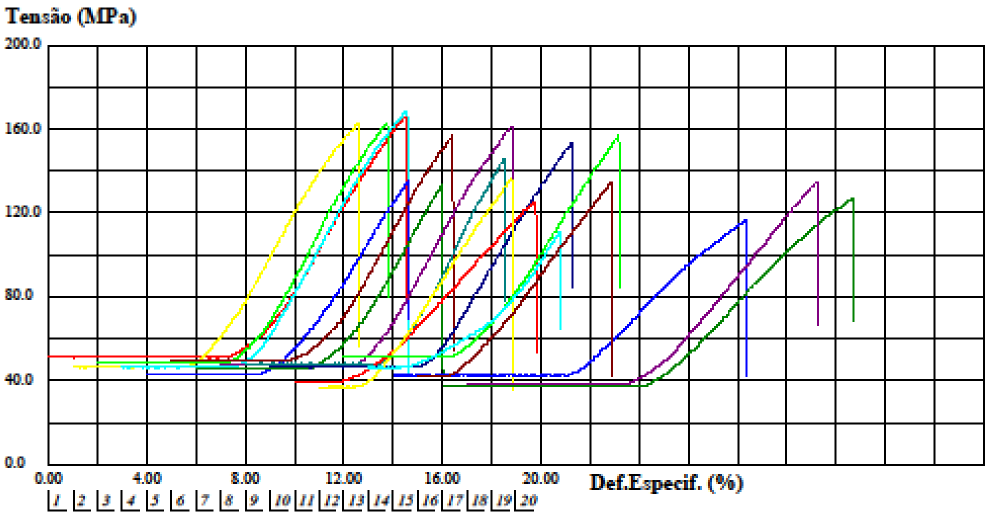

---

* Alguns grupos apresentam mais de dezoito espécimes testados, pois alguns espécimes apresentaram falhas em sua estrutura, necessitando de repetição.

Grupo 1%

UFPEL ensaio de flexão 3 pontos

Relatório de Ensaio

Máquina: **Emic DL2000** Célula: **Trd 24** Extensômetro: - Data: **16/10/2008** Hora: **10:26:22** Trabalho nº **0953**
Programa: **Tesc versão 3.01** Método de Ensaio: **Mini-Flexão 3 pontos**
Ident. Amostra: >> Grupo: **Luciano_G2**

Corpo de Prova	Area (mm2)	Tensão Máxima (MPa)	módulo elasticidade (MPa)
CP 1	0.58	156.91	1857.29
CP 2	0.60	162.42	1892.60
CP 3	0.61	157.01	1894.14
CP 4	0.58	162.12	1942.79
CP 5	0.59	152.07	1738.27
CP 6	0.60	142.79	1709.73
CP 7	0.60	146.07	1967.33
CP 8	0.58	149.99	1729.77
CP 9	0.59	134.56	1872.26
CP 10	0.60	145.64	1910.03
CP 11	0.66	156.84	1621.10
CP 12	0.59	148.54	1941.20
CP 13	0.68	140.38	1888.12
CP 14	0.75	150.72	1788.36
CP 15	0.62	169.00	1911.77
CP 16	0.65	163.46	1785.81
CP 17	0.59	147.46	1946.55
CP 18	0.68	149.49	1710.88
CP 19	0.62	133.21	1750.03
CP 20	0.60	152.52	1819.93
Número CPs	20	20	20
Média	0.6186	148.6	1849
Mediana	0.6023	150.4	1880
Desv.Padrão	0.04502	14.63	135.8
Coef.Var.(%)	7.277	9.851	7.345
Mínimo	0.5766	112.8	1575
Máximo	0.7534	169.0	2188

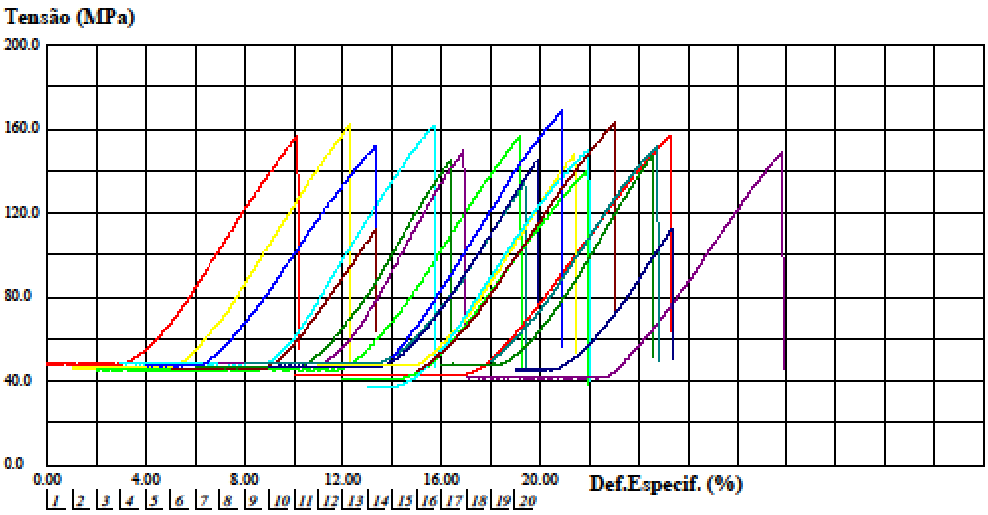

Grupo 2,5%

UFPEL ensaio de flexão 3 pontos

Relatório de Ensaio

Máquina: Emic DL2000 Célula: Trd 24 Extensômetro: - Data: 30/01/2008 Hora: 16:43:20 Trabalho nº 0966
Programa: Tesc versão 3.01 Método de Ensaio: Mini-Flexão 3 pontos
Ident. Amostra: >> Grupo: Luciano_G3

Corpo de Prova	Area (mm2)	Tensão Máxima (MPa)	módulo elasticidade (MPa)
CP 1	0.60	97.77	1463.96
CP 2	0.62	147.42	1996.80
CP 3	0.63	90.98	1619.16
CP 4	0.59	158.53	2108.43
CP 5	0.53	153.38	2391.64
CP 6	0.62	145.74	1988.90
CP 7	0.61	149.75	2076.26
CP 8	0.65	163.28	2254.41
CP 9	0.59	130.84	1866.80
CP 10	0.57	104.12	2000.88
CP 11	0.56	161.19	2071.40
CP 12	0.59	144.36	1763.96
CP 13	0.61	135.81	2074.78
CP 14	0.66	150.09	2162.34
CP 15	0.63	140.89	2017.19
CP 16	0.60	144.83	1804.65
CP 17	0.55	146.93	2368.20
CP 18	0.62	147.37	1884.62
CP 19	0.66	151.49	2009.40
Número CPs	19	19	19
Média	0.6044	136.6	1972
Mediana	0.6080	146.9	2009
Desv.Padrão	0.03553	25.51	277.5
Coef.Var.(%)	5.879	18.68	14.07
Mínimo	0.5259	74.36	1299
Máximo	0.6563	163.3	2392

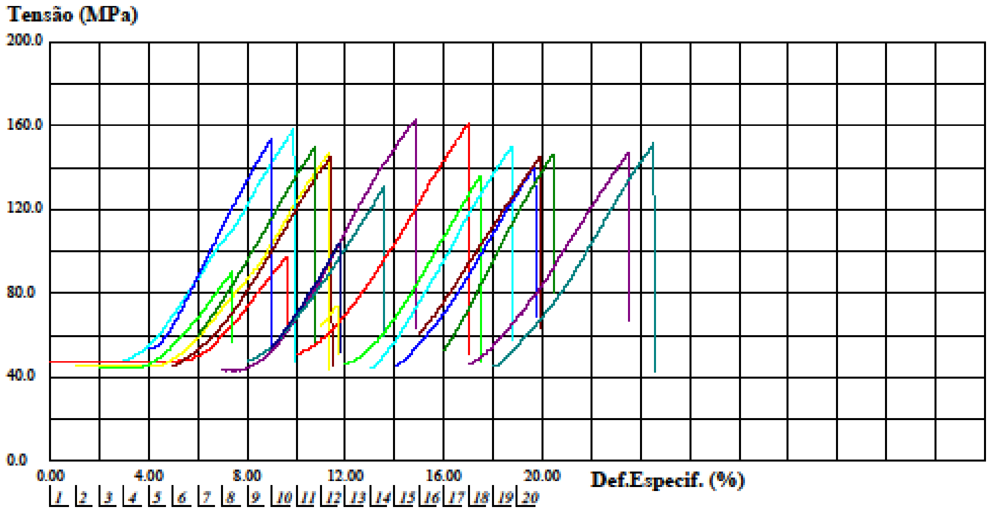

Grupo 5%

UFPEL ensaio de flexão 3 pontos

Relatório de Ensaio

Máquina: Emic DL2000 Célula: Trd 24 Extensômetro: - Data: 17/01/2008 Hora: 09:16:38 Trabalho nº 0957

Programa: Tesc versão 3.01 Método de Ensaio: Mini-Flexão 3 pontos

Ident. Amostra: >> Grupo: Luciano_G4

Corpo de Prova	Área (mm2)	Tensão Máxima (MPa)	módulo elasticidade (MPa)
CP 1	0.73	113.03	1693.87
CP 2	0.73	119.70	1840.23
CP 3	0.79	125.39	1718.09
CP 4	0.65	148.20	1831.14
CP 5	0.64	144.66	1894.37
CP 6	0.65	132.22	1708.91
CP 7	0.61	142.50	1714.32
CP 8	0.77	124.41	1686.77
CP 9	0.66	143.52	1635.06
CP 10	0.63	140.46	1902.30
CP 11	0.56	159.71	2138.66
CP 12	0.63	148.88	1819.12
CP 13	0.66	112.82	1970.95
CP 14	0.74	132.96	1535.02
CP 15	0.71	111.46	1659.22
CP 16	0.73	124.75	1562.47
CP 17	0.69	132.38	1896.98
CP 18	0.71	134.74	1637.07
CP 19	0.67	130.91	1732.72
Número CPs	19	19	19
Média	0.6825	133.8	1758
Mediana	0.6691	132.4	1718
Desv.Padrão	0.05914	14.93	159.6
Coef.Var.(%)	8.666	11.15	9.078
Mínimo	0.5603	111.5	1530
Máximo	0.7938	162.5	2139

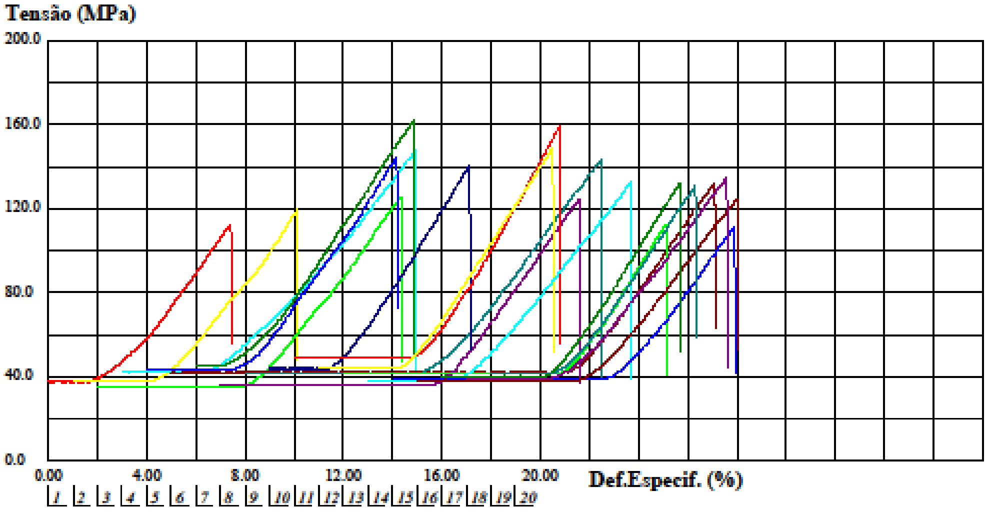

Grupo 10%

UFPEL ensaio de flexão 3 pontos

Relatório de Ensaio

Máquina: Emic DL2000 Célula: Trd 24 Extensômetro: - Data: 18/01/2008 Hora: 10:21:34 Trabalho nº 0958
Programa: Tesc versão 3.01 Método de Ensaio: Mini-Flexão 3 pontos
Ident. Amostra: >> Grupo: Luciano_G5

Corpo de Prova	Area (mm2)	Tensão Máxima (MPa)	módulo elasticidade (MPa)
CP 1	0.73	127.48	1476.15
CP 2	0.66	135.31	1894.63
CP 3	0.71	144.87	1634.94
CP 4	0.73	121.67	1746.24
CP 5	0.73	148.13	1578.24
CP 6	0.81	114.79	1412.64
CP 7	0.70	127.03	1590.76
CP 8	0.68	143.47	1740.58
CP 9	0.69	134.05	1571.00
CP 10	0.69	153.51	1700.41
CP 11	0.78	103.11	1453.55
CP 12	0.66	119.77	1703.48
CP 13	0.82	122.41	1407.72
CP 14	0.84	128.90	1516.00
CP 15	0.68	137.73	1719.33
CP 16	0.73	116.58	1733.59
CP 17	0.73	128.17	1762.18
CP 18	0.79	131.15	1413.58
CP 19	0.67	139.95	1670.51
Número CPs	19	19	19
Média	0.7269	128.8	1645
Mediana	0.7280	128.9	1671
Desv.Padrão	0.05487	14.72	162.5
Coef.Var.(%)	7.548	11.42	9.881
Mínimo	0.6563	97.48	1408
Máximo	0.8353	153.5	2005

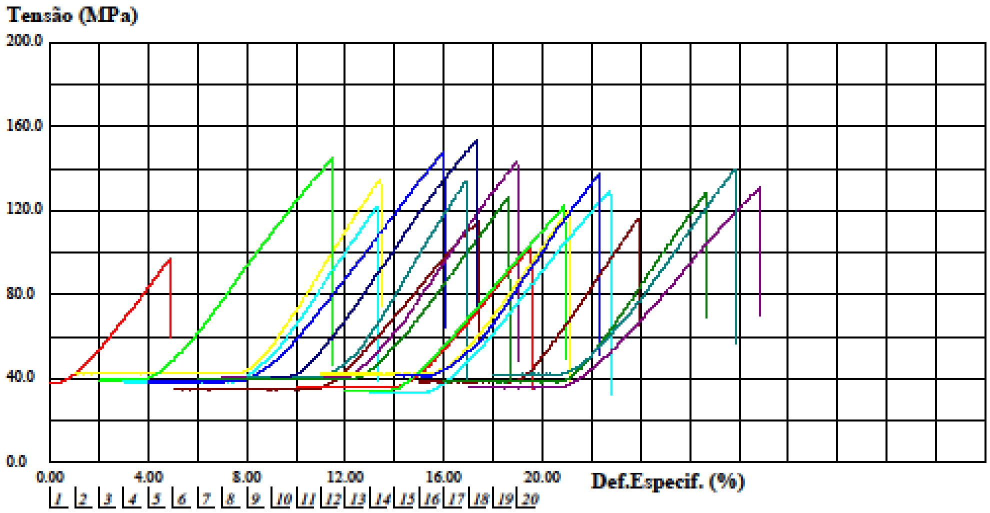

Relatório do ensaio de microdureza

Nanopartículas	Corpo de Prova	Leituras (kgf/mm^2)			Média (kgf/mm^2)
0%	1	37,4	36,0	33,2	35,5
	2	32,2	33,7	37,2	34,4
	3	36,1	30,2	32,9	33,1
	4	31,7	51,2	26,5	36,5
	5	42,8	34,9	34,5	37,4
1%	1	31,2	33,3	46,6	37,0
	2	44,4	34,8	36,8	38,7
	3	35,0	43,8	53,0	43,9
	4	28,4	34,5	47,3	36,7
	5	36,8	29,3	30,6	32,2
2,5%	1	34,8	38,7	28,6	34,0
	2	38,8	49,6	29,0	39,1
	3	39,2	35,9	35,7	36,9
	4	30,7	39,7	32,7	34,4
	5	39,8	35,9	28,9	34,8
5%	1	45,7	42,1	58,3	48,7
	2	47,2	33,2	40,1	40,2
	3	38,7	37,2	42,4	39,4
	4	42,3	50,3	47,2	46,6
	5	44,0	43,0	51,8	46,3
10%	1	40,3	37,4	39,7	39,1
	2	42,6	49,5	43,6	45,2
	3	44,9	47,3	43,5	45,2
	4	40,6	41,7	32,6	38,3
	5	48,5	49,4	37,4	45,1

Relatório da avaliação da espessura de película

Amostras	Nanopartículas				
	0%	**1%**	**2,5%**	**5%**	**10%**
1ª	20	22	38	40	48
2ª	16	22	32	33	42
3ª	23	18	16	48	42
4ª	29	34	45	37	54
5ª	38	36	34	41	58

Valores em µm.

Apêndice B – Relatórios dos ensaios referentes ao Artigo 2.

Relatório da avaliação do grau de conversão.

Amostras	Tratamento de partículas			
	Controle	Silano	Monômero ácido carboxilado	Monômero ácido fosforado
1ª	59,66	53,94	53,18	53,95
2ª	59,11	54,38	60,29	57,21
3ª	58,69	54,89	49,97	61,63
4ª	57,90	53,56	63,62	62,25
5ª	59,54	53,85	63,63	63,50

Valores em porcentagem (%).

Relatórios do ensaio de resistência à mini-flexão e módulo de elasticidade

Controle

UFPEL ensaio de flexão 3 pontos

Relatório de Ensaio

Máquina: Emic DL2000 Célula: Trd 24 Extensômetro: - Data: 26/04/2008 Hora: 12:43:25 Trabalho n° 1146
Programa: Tesc versão 3.01 Método de Ensaio: Mini-Flexão 3 pontos
Ident. Amostra: >>Grupo: controle

Corpo de Prova	Área (mm2)	Tensão Máxima (MPa)	módulo elasticidade (MPa)
CP 1	0.71	35.88	1762.88
CP 2	0.79	41.24	1434.58
CP 3	0.78	29.91	1228.93
CP 4	0.74	41.05	1623.81
CP 5	0.72	41.81	1386.72
CP 6	0.78	43.98	1638.47
CP 7	0.70	42.72	1585.63
CP 8	0.70	38.38	1499.79
CP 9	0.77	39.04	1653.06
CP 10	0.63	35.68	1685.10
CP 11	0.70	49.02	1808.69
CP 12	0.75	43.01	1847.31
CP 13	0.73	41.22	1595.52
CP 14	0.71	34.92	1633.86
CP 15	0.72	39.17	1719.31
CP 16	0.78	35.99	1544.12
CP 17	0.76	45.50	1676.85
CP 18	0.76	41.90	1759.29
CP 19	0.90	37.51	923.48
CP 20	0.77	35.00	1069.25
Número CPs	20	20	20
Média	0.7456	39.65	1554
Mediana	0.7474	40.11	1629
Desv.Padrão	0.05229	4.396	241.8
Coef.Var.(%)	7.014	11.09	15.56
Mínimo	0.6307	29.91	923.5
Máximo	0.8954	49.02	1847

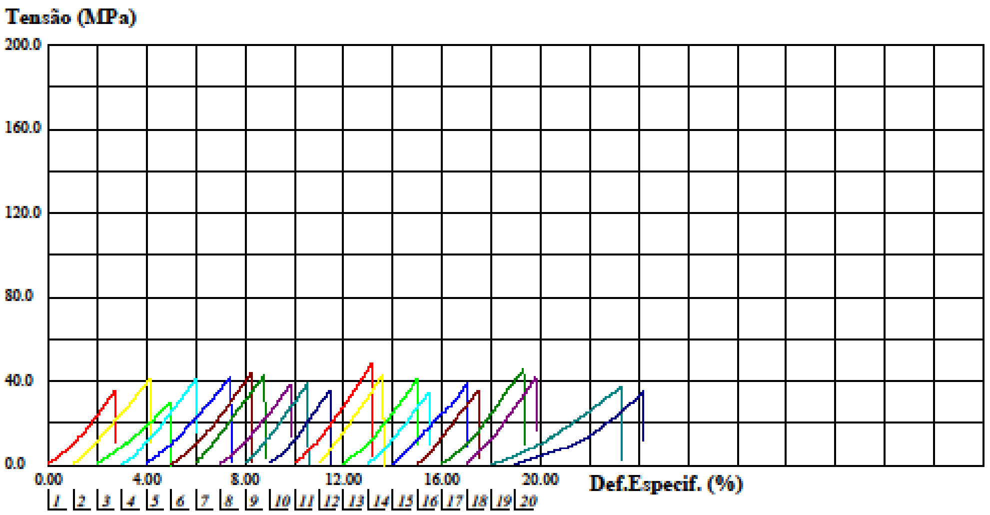

Silano

UFPEL ensaio de flexão 3 pontos

Relatório de Ensaio

Máquina: Emic DL2000 Célula: Trd 24 Extensômetro: - Data: 26/04/2008 Hora: 09:58:17 Trabalho nº 1145
Programa: Tesc versão 3.01 Método de Ensaio: Mini-Flexão 3 pontos
Ident. Amostra: >>>Grupo: G1

Corpo de Prova	Área (mm2)	Tensão Máxima (MPa)	módulo elasticidade (MPa)
CP 1	0.61	90.11	2142.24
CP 2	0.64	108.13	1973.27
CP 3	0.64	132.06	2122.92
CP 4	0.60	117.94	2398.79
CP 5	0.64	98.81	1954.09
CP 6	0.65	91.87	1915.11
CP 7	0.68	99.01	1840.33
CP 8	0.69	101.38	1740.62
CP 9	0.74	101.43	1853.02
CP 10	0.64	95.21	1995.42
CP 11	0.66	108.59	2078.91
CP 12	0.57	123.30	2195.25
CP 13	0.63	123.44	2024.80
CP 14	0.64	95.50	2096.03
CP 15	0.64	113.05	1950.36
CP 16	0.66	88.48	1895.01
CP 17	0.62	86.16	2399.51
CP 18	0.68	99.03	1958.59
CP 19	0.61	134.16	2077.19
CP 20	0.62	135.63	2211.20
Número CPs	21	20	20
Média	0.6434	107.2	2041
Mediana	0.6403	101.4	2010
Desv.Padrão	0.03545	15.73	172.4
Coef.Var.(%)	5.511	14.68	8.445
Mínimo	0.5714	86.16	1741
Máximo	0.7356	135.6	2400

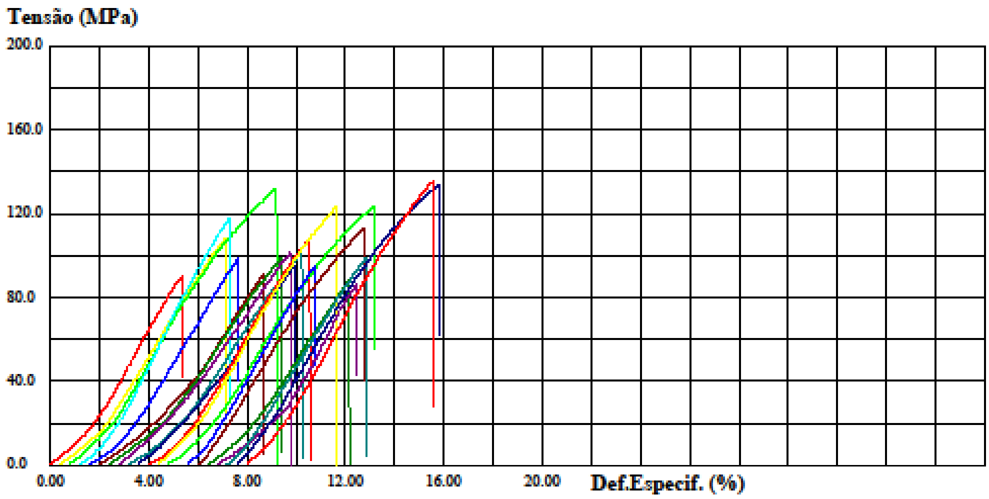

Monômero ácido carboxilado

UFPEL ensaio de flexão 3 pontos

Relatório de Ensaio

Máquina: Emic DL2000 Célula: Trd 24 Extensômetro: - Data: 26/04/2008 Hora: 09:19:41 Trabalho n° 1144

Programa: Tesc versão 3.01 Método de Ensaio: Mini-Flexão 3 pontos

Ident. Amostra: >>>Grupo: G2

Corpo de Prova	Area (mm2)	Tensão Máxima (MPa)	módulo elasticidade (MPa)
CP 1	0.79	36.82	1155.12
CP 2	0.64	49.77	1699.20
CP 3	0.68	61.67	1567.55
CP 4	0.66	60.35	1738.64
CP 5	0.70	47.96	1680.12
CP 6	0.70	62.21	1685.07
CP 7	0.65	64.19	1782.23
CP 8	0.63	49.44	1958.13
CP 9	0.69	49.68	1596.64
CP 10	0.65	47.53	1776.54
CP 11	0.66	57.18	1902.50
CP 12	0.66	89.03	2042.23
CP 13	0.67	51.16	1798.91
CP 14	0.67	59.65	1821.95
CP 15	0.65	46.63	1651.97
CP 16	0.68	79.98	2034.88
CP 17	0.75	48.02	1575.21
CP 18	0.65	46.60	1625.22
CP 19	0.68	59.53	1754.03
CP 20	0.70	56.84	1586.28
Número CPs	20	20	20
Média	0.6785	56.21	1722
Mediana	0.6716	54.00	1719
Desv.Padrão	0.03744	12.01	196.2
Coef.Var.(%)	5.517	21.36	11.40
Mínimo	0.6267	36.82	1155
Máximo	0.7851	89.03	2042

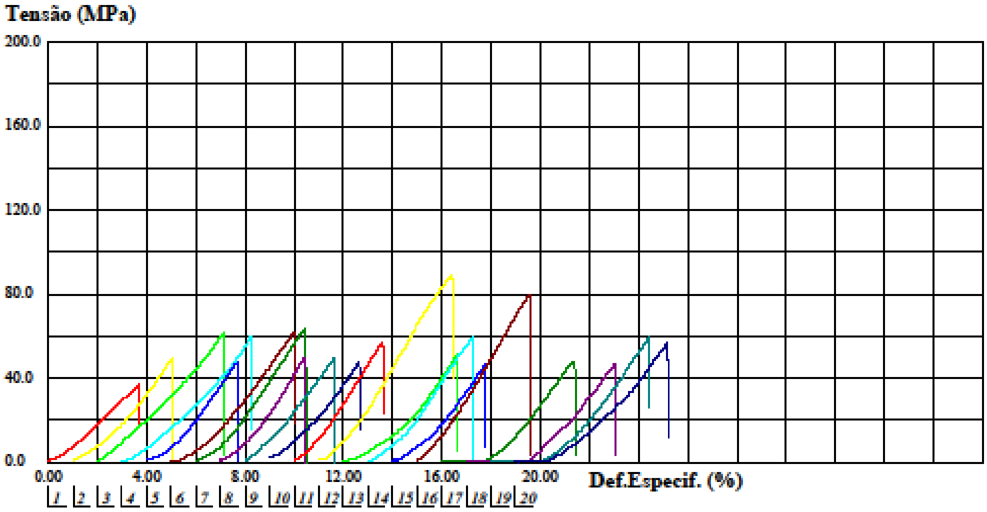

Monômero ácido fosforado

UFPEL-FO-CDC BIOMATERIAIS ensaio de flexão 3 pontos

Relatório de Ensaio

Máquina: Emic DL2000 Célula: Trd 24 Extensômetro: - Data: 07/05/2008 Hora: 16:51:55 Trabalho nº 1153
Programa: Tesc versão 3.01 Método de Ensaio: Mini-Flexão 3 pontos
Ident. Amostra: >> Grupo:

Corpo de Prova	Área (mm2)	Tensão Máxima (MPa)	módulo elasticidade (MPa)
CP 1	0.73	27.36	894.99
CP 2	0.67	22.88	859.77
CP 3	0.78	20.09	764.82
CP 4	0.69	22.01	807.40
CP 5	0.75	23.23	729.75
CP 6	0.81	18.40	704.61
CP 7	0.69	28.17	819.08
CP 8	0.83	25.09	742.53
CP 9	0.80	24.05	883.04
CP 10	0.81	24.26	799.35
CP 11	0.76	20.25	726.54
CP 12	0.64	21.13	851.58
CP 13	0.85	21.71	643.56
CP 14	0.72	24.15	824.31
CP 15	0.79	20.98	747.64
CP 16	0.79	24.24	672.40
CP 17	0.78	29.37	825.71
CP 18	0.80	15.57	731.31
CP 19	0.66	28.50	864.81
CP 20	0.78	20.36	814.70
Número CPs	20	20	20
Média	0.7554	23.09	785.4
Mediana	0.7767	23.05	803.4
Desv.Padrão	0.06080	3.524	71.14
Coef.Var.(%)	8.049	15.26	9.058
Mínimo	0.6390	15.57	643.6
Máximo	0.8533	29.37	895.0

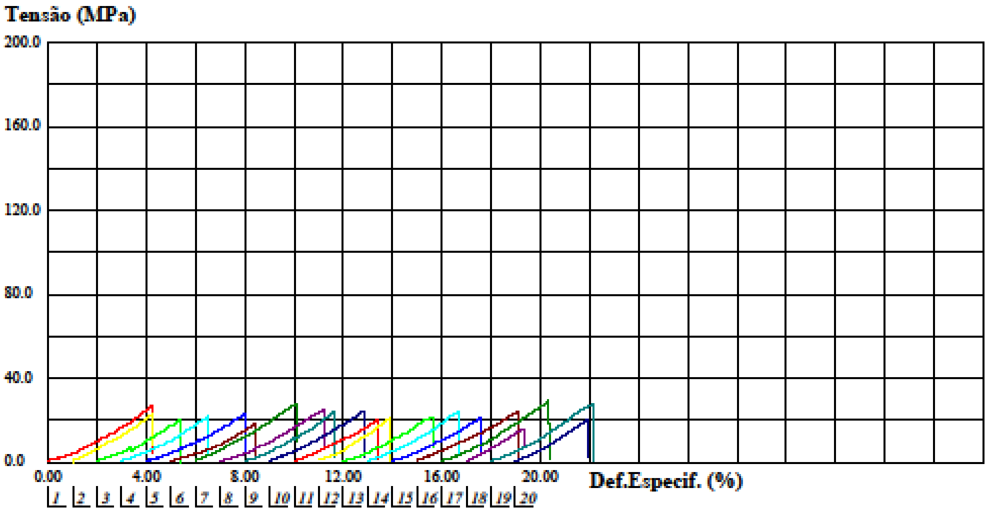

Relatório do ensaio de microdureza

Grupo	Corpo de Prova	Leituras (kgf/mm^2)			Média (kgf/mm^2)
Controle	1	15,6	17,4	14,5	15,9
	2	16,5	13,2	13,9	14,6
	3	19,2	15,3	17,8	17,5
	4	17,6	15,9	17,8	17,1
	5	19,2	17,5	20,4	19,0
Silano	1	32,8	32,7	34,8	33,4
	2	39,6	37,1	37,4	38,0
	3	31,2	33,7	31,5	32,1
	4	36,9	33,2	34,1	34,7
	5	36,2	32,7	33,5	34,1
Monômero ácido carboxilado	1	26,0	25,0	24,5	25,2
	2	23,1	25,1	23,1	23,8
	3	26,0	23,1	23,1	24,1
	4	24,0	22,5	22,3	22,9
	5	21,0	22,8	21,9	21,9
Monômero ácido fosforado	1	14,3	20,1	15,2	16,5
	2	17,7	18,7	19,2	18,5
	3	20,6	20,3	20,2	20,4
	4	18,7	16,9	16,8	17,5
	5	15,8	18,7	19,3	17,9

Relatório da avaliação da espessura de película

Amostras	Tratamento de partículas			
	Controle	Silano	Monômero ácido carboxilado	Monômero ácido fosforado
1ª	8	6	17	44
2ª	12	7	15	41
3ª	9	1	20	38
4ª	10	2	21	34
5ª	12	5	13	36

Valores em µm.